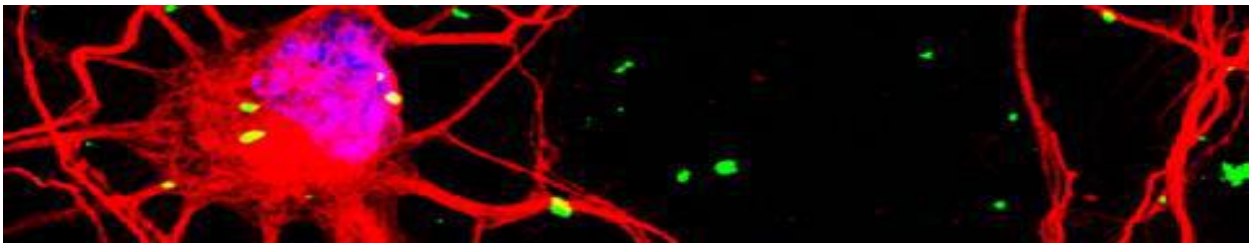

Doctoral School in Neuroscience
Curriculum "Neuroscience and Brain Technologies"
XXXII Cycle

"A novel chemo-optogenetic nanomachine sensitive to intracellular pH shifts"

Candidate: **Assunta Merolla**

Supervisors: **Fabio Benfenati, MD**

Fabrizia Cesca, PhD

UNIVERSITÀ DEGLI STUDI
DI GENOVA

iit NSYN ISTITUTO ITALIANO DI TECNOLOGIA
SYNAPTIC NEUROSCIENCE

Contents

Abstract

Epilepsy is a neurological disorder characterized by repeated seizures. Nowadays drugs and other approaches to reduce them are available but, unfortunately, around 30% of patients do not respond to medical therapies. In the last decade, optogenetics has emerged as a tool to both explore neuronal networks dynamics and to treat neurological conditions such as epilepsy. The optogenetics strategy involves the expression, in precise brain areas, of light sensitive proteins called opsins that are able to change the membrane potential upon wavelength-specific illumination. This last aspect is, usually, achieved using LED-based hardware. Despite the many advantages of this technique, it still faces practical and translational challenges because of the difficulties of illuminating multiple and deep areas of the brain. In this scenario, the search of alternative light sources is a goal to achieve. Luciferases are enzymes able to emit light upon addittion of their own substrate coelenterazine, and can be used to deliver light to opsins and modulate their action. In this work, the probe called *pHIL* (pH sensitive inhibitory luminopsin) was developed with the purpose to modulate the epileptic phenotype. pHIL is composed of a bioluminescent protein, RLuc8, coupled to the inhibitory opsin eNpHR3.0. Moreover, the control of seizures will occur only under the intracellular acidic conditions observed in epileptic neurons. The pH sensitivity of the probe is given by the presence of a pH sensor, a pH-sensitive variant of EGFP, called E^2GFP. The functioning of the probe is based on the BRET mechanism. The UV light that comes from the luciferase is transferred to the E^2GFP that under acidic conditions will emit light and activate the eNpHR3.0, promoting membrane hyperpolarization of epileptic neurons. pHIL is expressed and localizes at the plasma membrane in both HEK293T cells and primary hippocampal neurons. Moreover, pHIL hyperpolarizes HEK293T

under acidic conditions and upon addition of CTZ 400a, the specific luciferase substrate able to induce UV light emission. On the basis of our data, therefore, we propose pHIL as a potential therapeutic tool to counteract neuronal hyperexcitability.

1 Introduction

1.1 Neuronal excitability and pH.

Brain cells are highly sensitive to a vast number of chemical factors, either exogenous such as drugs or toxins, or intrinsic such as neurotransmitters and hormones. One of the most important intrinsic neuromodulator is the H^+ ion that can influence, in a very powerful way, neuronal function. The negative logarithm of H^+ ion concentration (pH) is a fundamental cellular parameter that is critical to a series of processes including cell division, metabolism, apoptosis, and cell migration[1–3] but also neuronal function and, in particular, synaptic transmission.

The central role of pH in the control of synaptic transmission depends on the high pH sensitivity of a large number of molecules including various types of voltage and ligand gated channels, ion pumps and carriers. At the presynaptic side, for instance, it is known that the initial rise in the presynaptic calcium concentration mediated via voltage-gated calcium channels is pH dependent, as the opening and the conductivity of presynaptic voltage-gated calcium channels strongly depends on both extracellular and intracellular pH[4]. Protons bind sensors near the pore of the channel, thus reducing channel conductance and shift the channel activation voltage to more positive values. A central role in the increase of presynaptic calcium coming from intracellular stores is played by inositol 1,4,5-trisphosphate[5] and ryanodine receptors[6], whose activity is strongly pH dependent.

At the postsynaptic side, instead, the N-methyl-D-aspartate-sensitive ionotropic glutamate receptors (NMDARs) are strongly modulated by changes in extracellular pH: a decrease in extracellular pH inhibits the ion channel function; on the contrary, an increase of extracellular pH activates the channel[7]. In contrast, kinetics and amplitudes of α-amino-3-hydroxy-5-methyl-4-isoxazolepropionic acid (AMPA) and

Kainate receptors-mediated currents are only marginally modulated by alteration of extracellular pH. In this respect, protons inhibit AMPA receptor function by enhancing receptor desensitization[8]. In addition, γ-aminobutyric acid (GABA) receptor activity is modulated by pH. $GABA_A$ receptor-mediated currents are enlarged at low extracellular pH, whereas a high pH inhibits the GABA response[9]. $GABA_A$ receptors are also permeable to bicarbonate ions (HCO_3^-). In contrast to the direction of chloride fluxes, which vary depending on the existing chloride gradients, modulated by the cation-chloride co-transporters NKCC1 and KCC2, the existing gradients always drive HCO_3^- out of the neurons under physiological conditions. Therefore, the opening of a $GABA_A$ channel will result in an HCO_3^- efflux, leading to intracellular acidification and extracellular alkalization. Consequently, GABAergic transmission itself can cause alterations of both intra- and extracellular pH.

From these and other evidences it is therefore clear that pH modulates neuronal excitability. Thus, the pH homeostasis in the brain must be tightly regulated.

1.2 Regulation of pH homeostasis in the brain.

Cellular pH homeostasis is established by active transport or buffering. Steady state intracellular pH (pH_i) is dependent on the balance between the rate of acid loading and the rate of acid extrusion. In neurons acid loading processes are able to restore the steady state pH_i after alkalinization and consist in the accumulation of H^+ generated through anaerobic or aerobic metabolism during neuronal firing or in the extrusion of HCO_3^- from cells thanks to the action of Cl-HCO3 exchangers, mainly the Anion Exchanger 3 (AE3), which typically extrudes HCO_3^- in exchange for extracellular Cl^-. Acid extrusion, on the contrary, is a process that tends to raise pH_i and in neurons it is usually achieved by the action of the SLC4 and SLC9 families of

Na^+-coupled transport proteins. These transporter families take advantage of the Na^+ inward gradient established by the Na^+/K^+ ATPase to extrude H^+ from the cell or accumulate a weak base (HCO_3^-) in the intracellular side (in the case of Na^+/HCO_3^- cotransporters). The main H^+ extruder is the Na^+/H^+ Exchanger Type 1 (NHE1). It is expressed in all mammalian cell types and is a primary regulator of intracellular pH homeostasis and cell volume[10]. The major function of NHE1 is to contrast excessive intracellular acidification and maintain the acid–base balance in the cytoplasm. In hippocampal and cortical neurons, NHE1 is mainly activated by a decrease in intracellular pH[11]. When intracellular acidosis occurs, NHE1 activation is indispensable for the extrusion of H^+ to restore the physiological intracellular pH. Na^+/HCO_3^- co-transporters also mediate acid extrusion. The co-transporter Slc4a4 and Slc4a7 are expressed in the nervous system; in particular, Slc4a7 is shown to co-localize with PSD-95, a postsynaptic protein of glutamatergic synapses, and its expression is increased upon metabolic acidosis[12].

The importance of acid loaders and extruders in the maintenance of neuronal homeostasis is underlined when phenotypes of transporters or exchangers knock out mice are observed. It is known that AE3-null mice show a greater seizure-induced mortality consistent with enhanced neuronal excitability, also NHE1-null mice are characterized by increased Na^+ currents in hippocampal neurons and, as a consequence, by higher excitability resulting in epileptic seizures[13,14]. Thus, there is a reciprocal relationship between neuronal activity and sizable shifts in intracellular pH[15,16]. Given this reciprocal relationship, tools to accurately measure hydrogen ion concentration are important for understanding the role that pH plays during the evolution of both physiological and pathological network states.

1.3 Methods to measure H^+ concentration.

The first method used to monitor intracellular pH changes involved the use of pH-sensitive glass electrodes inserted into individual 500-600 µm muscle fibres of the crab, *Carcinus maenas*, for the determination of their intracellular pH[17].pH sensitive dyes were subsequently developed and, with the discovery of Green Fluorescence Protein (GFP), pH sensitive GFP variants were developed. Dyes and engineered GFP based pH indicators can be classified into two general families: non-ratiometric and ratiometric. Among the *non-ratiometric pH sensitive GFP-based probes*, the "Ecliptic" and "Superecliptic" pHluorins are the most widely employed[18,19].These GFP variants gradually lose fluorescence as pH is lowered, until at pH values of <6.0, the excitation peak at 475 nm vanishes. In an environment of pH <6.0, the protein is invisible (eclipsed) under 475-nm excitation but can be seen at 395 nm. These changes are reversible within 20 ms after returning to neutral pH[18] .Ecliptic and superecliptic pHluorins were applied to investigate the exocytosis of presynaptic vesicles. Targeted expression of ecliptic and superecliptic pHluorin to acidic secretory vesicles allows the real-time analysis of the exocytotic fusion of these vesicles to the plasma membrane, as when the pH becomes neutral, there is a correspondent increase in fluorescence. pHluorins are thus ideal for the analysis of exocytosis, however over time a loss of florescence is observed, due to transit from the neutral extracellular environment to an acidic vesicle or to the proteolytic breakdown of these tagged proteins in lysosomes, leading to confounding analyses. Moreover, the equilibrium between the protonated and deprotonated states of these proteins is also affected by temperature and ionic strength. Furthermore, the light emitted by such sensor proteins is dependent on their concentration. The latter problem was resolved thanks to the introduction of *ratiometric pH sensitive dyes and*

GFP-based probes, which are differentially sensitive to the analytes for at least two excitation or emission wavelengths. For instance, for a suitable fluorescent dye, emission at one chosen wavelength may be enhanced or diminished relative to the emission at another wavelength. The use of ratiometric pH sensors requires calibration to characterize the relationship between the fluorescence properties of the sensor and pH. The calibration can be carried out adding high K^+ buffers at different pH together with ionophores such as the K^+/H^+ exchanger nigericin to equilibrate intracellular and extracellular pH. Fluorescence intensities are used to determine ratios and by collecting fluorescence ratios at known different pH, a curve can be constructed. Interpolating ratio values in this curve, unknown pH_i values can be extrapolated. The pH-sensitive ratiometric dyes BCECF-AM (2',7'-Bis-(2-Carboxyethyl)-5-(and-6)-Carboxyfluorescein Acetoxymethyl Ester) and SNARF-AM (seminaphtorhodafluor-1-acetoxymethylester) acetoxymethyl ester, are routinely used to determine pH_i. The presence of a methyl ester makes both dyes membrane-permeant. Once the dye enters the cell, the methyl ester group is cleaved by intracellular esterases, which trap the dyes within cells. The dual-excitation/single-emission dye BCECF is characterized by a pH-sensitive excitation at 490 nm (λ_{em} 535 nm) and a pH insensitive excitation at 440 nm. The dual-emission dye SNARF has pH-sensitive and pH-insensitive emissions at 580 and 640 nm, respectively. The ratiometric measurement allows correction for dye leakage out of the cell, photobleaching, and differential dye loading between samples. One of the limitations of the use of these dyes is that their metabolism, leakage out of the cell, and photobleaching will all decrease the fluorescence intensity over time. For this reason, dyes are optimally used for short-term measurements.

The first ratiometric pH sensitive GFP was introduced by Miesenbock and his group in 1998. They found that a S202H GFP variant, named pHluorin, displayed a

bimodal excitation spectrum with peaks at 395 and 475 nm and an emission maximum at 509 nm[20] .Upon acidification, pHluorin excitation at 395 nm decreases with a corresponding increase in the excitation at 475 nm. Like ratiometric dyes, pHluorin is characterized by a pH-sensitive fluorescence with increased intensity at higher pH, and by a pH-insensitive fluorescence at the isosbestic excitation at 470 nm that can be used to normalize to biosensor abundance. This is different from what happens in the ecliptic pHluorin, in which the fluorescence increases with increasing pH at 410 nm excitation; however, its emission spectrum does not have an isosbestic point to normalize intensity to protein abundance. In 2002, Hanson and collaborators constructed a dual emission ratiometric pH sensitive GFP variant called deGFP4. This indicator responds to pH changes by opposing changes in blue and green emission. At a low pH, excitation of deGFP at 400 nm results in a blue fluorescence at 460 nm; at high pH, 400 nm excitation leads to green fluorescence at 516-518 nm[21]. As a final example, in 2006 the group of Dr. Bizzarri introduced the ratiometric pH sensitive GFP, *E^{2}GFP*, which contains four mutations with respect to GFPwt: F64L/S65T/T203Y/L231H. Thanks to these mutations, E^{2}GFP displays marked changes in both excitation and emission fluorescence spectra upon pH variations. When excited at 408 nm, E^{2}GFP shows higher fluorescence intensity at acidic pH compared to physiological pH, whereas when excited at 473 nm, E^{2}GFP shows the opposite behaviour[22]. These properties make the E^{2}GFP suitable to study the extracellular pH shifts during epileptic like conditions. Using this tool, Chiacchiaretta and colleagues demonstrated that, upon induction of neuronal hyperexcitability by convulsant drugs or high frequency electrical stimulation, extracellular acidification occurs at cell bodies and at synapses due to the activation of NHE1[23]. Recently, ratiometric GFP based probes were used by Raimondo and colleagues[24] to investigate the possibility for genetically encoded pH reporters to measure neuronal intracellular

pH transients associated with periods of elevated activity. The intracellular pH of individual pyramidal neurons within the CA1 and CA3 regions was measured using E^2GFP[22] and deGFP4[21]. Both pH sensors were able to report acidic shifts associated with epileptiform activity.

1.4 Seizures and epilepsy.

As said in previous paragraphs, a dysregulation of extra-intracellular pH homeostasis can induce pathological states like seizures and epilepsy. *Seizures* are temporary disruptions of brain function resulting from abnormal, excessive neuronal activity; epilepsy is a chronic condition of repeated seizures. Seizures can be classified in *generalized* and *focal* (or partial). A *generalized seizure* involves both hemispheres from the onset. *Focal seizures* originate instead in a small group of neurons, the seizure focus, which has enhanced excitability and the ability to spread that to other regions and cause a seizure.

How does enhanced excitability spread beyond the seizure focus? Each neuron in a seizure focus is characterized by sustained depolarization resulting in bursts of action potentials, followed by a rapid repolarization and hyperpolarization. This event is called *paroxysmal depolarizing shift*. The first depolarization phase depends primarily on the activation of AMPA and NMDA-type receptor channels and on the influx of extracellular Ca^{2+}, which leads to the opening of voltage-dependent Na^+ channels, influx of Na^+, and generation of repetitive action potentials. The NMDA-type channels are able to enhance excitability because depolarization allows the removal of the Mg^{2+} blockage of the channel. Once unblocked, the excitatory current through the channel increases, enhancing the depolarization and allowing extra Ca^{2+} to enter the neuron. The subsequent hyperpolarizing afterpotential is mediated by

GABA receptors and Cl^- influx, or by K^+ efflux. Hyperpolarization is important because it limits the duration of paroxysmal depolarizing shift. As long as the enhanced electrical activity is restricted within the focus there are no clinical manifestations. Usually, the abnormal activity is confined in a small group of neurons thanks to inhibitory effects of the excited region on surrounding tissue[26]. This *inhibitory surround* is dependent on the inhibition activity of GABAergic inhibitory interneurons. During a focal seizure, the inhibitory surround is overcome and the final hyperpolarization phase in the neurons of the focus disappears. The result is the spread of the seizure beyond the focus and the generation of continuous high frequency train of action potentials.

A very important factor in the spread of focal seizures is not only an increase of glutamatergic drive, but also a change in GABAergic effect. It is reported that an increase in postsynaptic chloride occur causing the shift of E_{GABA} to depolarizing levels. When the failure of the restraint period occur, the chloride loading is high because the membrane potential is shifted away from the resting E_{GABA} for the concurrent glutamatergic drive causing a larger GABAergic current[25].

An intense neuronal firing causes also the increase of extracellular levels of K^+ contributing to an increase of chloride loading because chloride clearance occurs through the KCC2 transporter that is controlled by the K^+ electrochemical gradient. A reduction of K^+ electrochemical gradient modifies the clearance of chloride[26] .

1.5 Animal models to study epilepsy and epileptic seizures.

In the world, the incidence of epilepsy is about the 1% of total population and the 30% of patients do not respond to conventional drug treatments. For this reason, several experimental animal models of epilepsy have been developed in which the

epileptic phenotype is simulated and different treatments are tested. These models are instrumental in the search for similarities with the mechanisms of human epilepsy. Animal models are subdivided in genetic and acquired, and the latter further subdivided into electrical or chemical induced[27]. Genetic animal models include animals with spontaneous or induced mutations resulting in recurrent seizures. For example, mutations in GluA4 AMPARs have been causally linked to absence seizures[28]. Electrical models like kindling are instead based on gradual development of seizures after repeated stimulation in initially healthy animals. In chemical induction models, pro-convulsants such as pentylenetrazol, kainic acid or bicuculline are injected into an animal to induce chronic seizures[27] or can be injected at high doses (for instance, pentylenetrazol injection) to reproduce acute seizures. These chemicals act on receptors critically involved in synaptic transmission, thereby disturbing the excitatory-inhibitory balance, enhancing excitation or blocking inhibition, and resulting in seizures. Chemical convulsants can be administered either intracerebrally or systemically.

Kainic acid (KA) is a cyclic analogue of L-glutamate and an agonist of ionotropic KA receptors. KA induces progressive limbic seizures mimicking human temporal lobe epilepsy (TLE). TLE symptoms consist of focal seizures that originate in the hippocampus, entorhinal cortex or amygdala many years after a brain injury like status epilepticus, encephalitis of febrile convulsions. Patients with TLE typically show hippocampal sclerosis with neuronal loss (for instance GABAergic interneurons) in the CA1/CA3 region of the hippocampus and the hilus, along with granule cell dispersion and aberrant mossy fiber sprouting in the molecular layer of the dentate gyrus. The hippocampus is indeed one brain region highly susceptible to neuropathological changes after either local or systemic administration of KA[29]. Intraventricular administration of KA preferentially damages the CA3 and CA4

regions of the hippocampus but leaves the CA1 region and the dentate gyrus almost intact. Intrahippocampal administration of KA produces CA3 pyramidal cell loss even if the injection is performed in distal regions such as CA1. Spontaneous seizures develop between 5 days to one month after the administration of KA in the hippocampus[30],. The pentylentetrazol (PTZ) model of epilepsy is considered similar to primary tonic-clonic generalized epilepsy in humans. PTZ is a $GABA_A$ receptor antagonist that produces severe convulsions when administered to animals. It mediates a loss of inhibition induced by GABA by specifically blocking $GABA_A$ receptors, as bicuculline is a competitive antagonist of $GABA_A$ receptors[31]. As an antagonist of the action of GABA neurotransmitter, bicuculline produces acute focused epileptic convulsions when administered systemically or when applied locally into the cortex. Bicuculline effects are evident within 1–5 min[32].

1.6 Possible options to treat seizures and epilepsy.

Therapies to treat epilepsy are available. In many cases, patients with epilepsy can lead a normal life thanks to antiepileptic drugs (AEDs). Many anticonvulsant drugs act by blocking excitation or enhancing inhibition. For example, benzodiazepines like diazepam and lorazepam enhance $GABA_A$-mediated inhibition, phenytoin and carbamazepine cause reduction in the opening of voltage gated Na^+ channels. However, despite progress in drug and epilepsy research, about 35% of all epileptic patients show recurrent spontaneous seizures that are refractory to AED administration. Drug resistance is a problem especially in patients with temporal lobe epilepsy, where seizures originate from the temporal lobe, mostly from the hippocampus, as said in the previous paragraph. Unfortunately, other treatment possibilities for drug resistant patients are limited. The ketogenic diet is a possibility

whose efficacy is however limited to some types of infantile epilepsies. Surgical intervention is another possibility and consists in the surgical resection of the seizure focus. For instance, amygdalohippocampectomy is usually performed for TLE. Unfortunately, a limited number of epilepsies are curable through surgery. Finally, another possible treatment is brain stimulation. Vagus nerve stimulation (VNS) is the most commonly used. In this procedure, a prosthesis is implanted under the skin of the patient chest. The stimulating electrodes carry intermittent electrical currents from the generator to the vagus nerve. The mechanism of action of VNS is not completely understood. It is possible that the activation of brain steam nuclei is involved, with projections in limbic, reticular and autonomic regions of the brain, the main targets of vagal afferents. In this context, the immunomodulatory function of the vagus nerve is very interesting. Afferent signals can activate the so-called cholinergic anti-inflammatory pathway upon inflammation. Through this pathway, efferent vagus nerve fibers inhibit the release of pro-inflammatory cytokines and in this way reduce inflammation, which plays an important role in seizures and epilepsy[33].

Despite important advancements, however, refractory epilepsies still represent a serious problem. For this reason, novel possible approaches for epilepsy treatment are being investigated, amongst them gene therapy. Gene therapy in the nervous system involves the transfer and expression of genes into brain tissue, which is possible thanks to the use of viral vectors like lenti-virus, adeno-associated virus (AAV), and herpes simplex virus (HSV) that allow long term gene expression without notable toxicity. The expression of therapeutic genes can be targeted to a specific cell type using specific promoters, specific virus serotypes or choosing a precise injection site. For epilepsy treatment, gene therapy can act through several mechanisms. For instance, it can modulate hyperexcitability by transduction of endogenous cells and expression of inhibitory modulators. One of the first therapeutic examples of using

viral vectors to constrain seizures was based on the bioactive neuropeptide galanin. Galanin is a 29-30 amino acid peptide highly distributed in the brain, especially in the septum and in locus coeruleus. The axons of the neurons located in these structures project to the hippocampus where the density of galanin receptors is high[34]. Physiological studies suggest that galanin has an inhibitory action in the hippocampus because it inhibits excitatory post-synaptic potentials (EPSPs) in pyramidal neurons of CA1[35]. For this reason galanin may have a modulatory effect on seizures. In some studies, AAV-mediated galanin overexpression suppressed intrahippocampal and intraperitoneal KA-induced seizures[36]. Another gene therapy-based strategy has been to decrease seizure-induced hyperexcitability by the expression of proteins called *opsins* to silence neuronal firing in excitatory cells or to induce firing in inhibitory cells. The use of opsins to modulate neuronal activity is the principle on which optogenetics is based.

1.7 A new way to modulate neuronal activity: optogenetics.

In recent years, a new technology called "optogenetics" has been introduced, which is based on the combination of optics and genetics. After the delivery of light sensitive opsin genes such as channelrhodopsin-2 (ChR2), halorhodopsin (NpHR) and others into the brain, excitation or inhibition of specific neurons in precise brain areas can be controlled by illumination at different wavelengths with very high temporal and spatial resolution. The development of such a revolutionary technique is due to the work of different research groups. For the first time Miesenbock and his group in 2002 developed the possibility to sensitize non-photoreceptor cells to light introducing in cultured mammalian neurons a combination of three proteins derived from *Drosophila melanogaster*. By using this system, called "chARGe", it was

possible to control the activity of cultured mammalian neurons[37]. Only after the discovery of Channelrhodopsin-2 (ChR2) from the algae, *Clamydomonas reinhardt* and Halorhodopsin (NpHR) from *Natromonas Pharaonis*, E. Boyden and K. Deisseroth developed the possibility to induce respectively the activation and the inhibition of neuronal activity with light[38,39]. When activated by a series of brief pulses of blue light, ChR2 channels open and allow the passive movement of Na^+, K^+, Ca^{2+} and H^+ following the electrochemical gradient[40]. Such ion flux leads to the net depolarization of the neuronal membrane, and if the cell is depolarized to threshold, action potentials are generated with millisecond timescale temporal resolution (Boyden et al., 2005). Instead, after illumination with green/yellow light, NpHR pumps Cl^- ions inside the cells mediating the inhibition of spike trains with high stability[39] .

The great advantage of optogenetics is the possibility to achieve cell-type specificity. Different cell types can be distinguished thanks to well-defined promoter activities. In this way, it is possible to target specific populations when they are interspersed among numerous other neuronal and non-neuronal cell types, for instance glial or endothelial cells. Another big advantage of optogenetics is the possibility of obtaining bidirectional control, as targeted neurons can be silenced or activated via different optogenetic probes. One disadvantage is linked to the illumination procedure. It is not possible to activate all brain cells at a given time point due to the limitations in the tissue volumes that can be illuminated at sufficient intensity. Only cells transduced and illuminated in a given tissue volume will be photosensitive, while cells that are not transduced or not sufficiently illuminated will be not photosensitive.

The potential to use optogenetics as therapeutic tool has been investigated since its early development. For example, optogenetics has been used to treat

neurodegenerative disorders, such as Parkinson's disease[41], as well as to treat non-neurological conditions such as ventricular tachycardia or ventricular fibrillation[42]. However, among the neurological disorders in which optogenetics can be applied, epilepsy is the best candidate. In epilepsy treatment, two optogenetics-mediated seizure-suppressant strategies can be used: silencing of endogenous excitatory cells, or activating endogenous GABAergic interneurons. Alternatively, these approaches can be combined and applied simultaneously and, alone or together, these strategies may normalize hyperexcitability in the epileptic foci in the brain.

1.8 Epileptic seizures control through optogenetics.

The activation of inhibitory interneurons involves the selective expression of ChR2 in GABAergic interneurons, which will mediate their activation upon blue light stimulation. This strategy was used to control a mixed population of interneurons by vesicular GABA transporter (VGAT) promoter-mediated ChR2 expression, and also to control fast-spiking interneurons by using parvalbumin (PV) promoter-driven ChR2 expression[43]. However, the effect of ChR2 can 'backfire' because the enhanced GABA release in some circumstances may increase synchronization of the network activity, and promote seizures[44]. Moreover, in some focal epilepsies like TLE a loss of interneurons is observed, which may reduce the effectiveness of this optogenetic approach.

The best way to shut down the excessive excitation that occurs during epileptic seizures is to induce the silencing of hyperexcited neurons. This strategy is possible thanks to the specific expression of the chloride pump *Natromonas Pharaonis* Halorhodopsin (NpHR)[45] in pyramidal neurons. The expression in this cell type can be mediated by a specific promoter like the Ca^{2+}/calmodulin-dependent protein kinase

II α (CaMKIIα). The photocycle kinetics of NpHR is on the millisecond scale, which allows fast neuronal inhibition resulting from hundreds of pA currents, readily translating into tens of mV hyperpolarization. Recently, in order to increase the rate of NpHR-mediated hyperpolarization, some groups worked to improve the halorhodopsin trafficking to the plasma membrane and to increase the export from the ER. For these purposes, an ER export sequence and a trafficking signal from the inward rectifying K^+ channel 2.1 (Kir2.1) were inserted at the C-terminal of the fusion protein. These modifications improved the surface membrane expression and photocurrents were profoundly increased in response to green/yellow light illumination. The new halorhodopsin variant was called *eNpHR3.0* [45]. Tønnesen and colleagues used eNpHR to hyperpolarize hyperexcited neurons in an in vitro model of epilepsy based on stimulation train-induced bursting in mouse hippocampal organotypic cultures, which in several ways is similar to pharmacoresistant human tissue from TLE patients. In these experiments eNpHR was specifically expressed in excitatory hippocampal neurons by introducing it in a lentiviral vector under the CaMKIIα promoter, which was injected directly into the hippocampus. This study demonstrated that the eNpHR expressed in hippocampal neurons, upon activation with yellow light, is capable of blocking epileptiform activity[46]. Another group used the halorhodopsin approach to study the in vivo suppression of epileptiform activity in the KA model of TLE. After light stimulation of precise neuron populations expressing NpHR, significant seizure control was achieved, stopping electrographic seizures and reducing the frequency of behavioural seizures [47].

1.9 Can optogenetics be applied in humans?

The different approaches for epilepsy treatment previously described require invasive brain surgery that is the only route of administration approved. This aspect can be a problem and the search for new ways of administration is a challenge. However, another aspect is to be taken in consideration. The very important concept at the basis of the optogenetic approach is the precise spatiotemporal wavelength-specific illumination. Despite poor light penetration in the brain tissue, implantable laser-coupled optical fibers or head mounted light emitting diodes (LEDs) are used for the delivery of light to the surface of the brain in awake and mobile animals. In humans, the situation will be different because of the larger brain areas to be illuminated. Conceivable strategies could be the construction of bundled optical fibers that branch out from the site of implantation or allow photons to escape from the side where the optical fiber is located. In these ways, the illumination volume is enlarged[48]. Recently, a multi electrode array coupled with an optical fiber has been constructed. This so called "optrode-MEA" device is able to deliver light to neural tissue and in the same time to record multisite extracellular activities from an area of 4.0 mm × 4.0 mm around the stimulation focus[49]. An upgrade of the "optrode-MEA" was developed in 2012. This new device is able to deliver optical excitation to a single cortical site while mapping the neural response from the surrounding 30 channels of the 6 × 6 element MEA for 8 month in chronically implanted ChR2 expressing rats[50]. The size of the last device is similar to the one used for the deep brain stimulation in clinical settings for patients, so it could be used in patients in any region of the brain enabling the illumination of larger brain areas. Although the development of strategies to enable optical fiber-mediated illumination of larger brain areas, chronically implanted optical fibers pose risks for infection and tissue damage.

Moreover, the transmission of external light through the brain is inefficient because of light scattering and tissue absorption. In fact, most of the light emitted by optical fibers is attenuated within 1 mm from the fiber tip[51].

In the last years, one potential solution to this issue has been addressed, i.e. to eliminate the need for an external light source by creating a system in which the animal produces its own light. The production of light in this case is due to the action of light-producing proteins that exist in nature, named *luciferases***.** These proteins can be expressed using viral systems in a way similar to the opsins, to internally generate light after the reaction with a specific substrate. In recent years, bioluminescence was applied in many molecular imaging applications in alternative to fluorescence imaging. In fluorescence imaging, photobleaching decreases signals over time while phototoxicity leads to damaged or dead cells due to light-induced generation of free radicals[52]. Both these phenomena are non-existent in bioluminescence. These features make the bioluminescence a potentially good tool for light delivery in optogenetics applications.

1.10 Bioluminescence and optogenetics.

In a bioluminescence-based optogenetic system, light is generated by the luciferase to activate the opsin, resulting in the activation (in case of channelrhodopsins) or inhibition (in case of proton or chloride pumps) of the target neurons. For the first time Berglund and colleagues managed to activate ChR2 using the *Gaussia* Luciferase (GLuc) light. In this case ChR2 could be activated directly by illumination, but also chemically by the luciferase substrate, *coelenterazine*. Coelenterazine is oxidized by GLuc to generate bioluminescence that peaks at 470 nm, which matches the excitation spectrum of ChR2[53]. Other groups tried to use a

combination of opsins and luciferases to modulate neuronal activity. For example Land et al. used the Firefly luciferase (FLuc) in combination with NpHR in order to obtain the inhibition of neuronal activity. FLuc produces yellow-red light in the presence of its substrate, luciferin[54]. Notably, the emission spectrum of firefly luciferase overlaps highly with the action spectrum of NpHR. This suggests that with sufficient light output, luciferase could serve as a light source that would activate halorhodopsin and inhibit neural activity, eliminating the need for an external light source[55]. However, the bioluminescent signal is 10^3 times lower than the fluorescent signal[52] and the light output from luciferases is insufficient to provide temporal and spatial resolution equivalent to fluorescence so when it is applied to optogenetics, the hyperpolarization/depolarization rate is low. The problem of low brightness has been solved in nature by the phenomenon of *bioluminescence resonance energy transfer (BRET)*, in which the emitted light coming from the reaction of the luciferase with its specific substrate excites a fluorescent protein increasing the number of emitted photons. There are many types of luciferases, such as the above-mentioned Firefly and Gaussia Luciferase, but the luciferase utilized as a BRET donor is mainly *Renilla luciferase (RLuc)*. Renilla luciferase is the most used because it is not ATP dependent and in general requires only molecular oxygen in addition to its substrate, *the coelenterazine (CTZ)*, for luminescence. The limiting factors of RLuc reaction are its rapid inactivation and low brightness. To improve RLuc characteristics, site directed mutagenesis of the RLuc gene and chemical synthesis of analogues of the coelenterazine were performed[56,57] .Combining RLuc variants and coelenterazine analogues, a variation of the wavelength of RLuc emission spectrum is also possible. This last aspect is very important in BRET, in order to obtain different donor emission spectra for the excitation of various fluorescent proteins. The first RLuc variant, obtained by Loening et al., was called *RLuc8*. It presented eight mutations

(A55T, C124A, S130A, K136R, A143M, M185V, M253L, and S287L) and exhibited a 200-fold improvement in resistance to murine serum inactivation at 37°C, a 4-fold improvement in light output, and a 5-nm red shift in the emission spectrum in comparison with the native RLuc. However for imaging bioluminescent reporters in animals, RLuc variants with an emission from red to near infrared wavelength were needed. Thus, several red shifted variants were obtained by random mutagenesis of luciferase proteins and upon the reaction with coelenterazine analogues. Mutants with maxima in the yellow and yellow-orange region were obtained, characterized by high stability and brightness[56]. As said before, chemical synthesis of coelenterazine analogues was performed for the optimization of RLuc emission. During the 70s several coelenterazine analogues were synthesized, including *coelenterazine h* and *coelenterazine 400a*[58]. Coelenterazine h, when reacting with RLuc emits light at a wavelength of 470-480 nm with a 10 to 20 fold higher luminescent intensity of that of native coelenterazine. Coelenterazine 400a is very used in BRET studies because it emits at 390 - 400 nm that has minimal overlapping with the emission of the GFP acceptor. Over the years, more coelenterazine variants have been modified in order to obtain a better stability and a controlled reaction with the enzyme **[Figure 1]**.

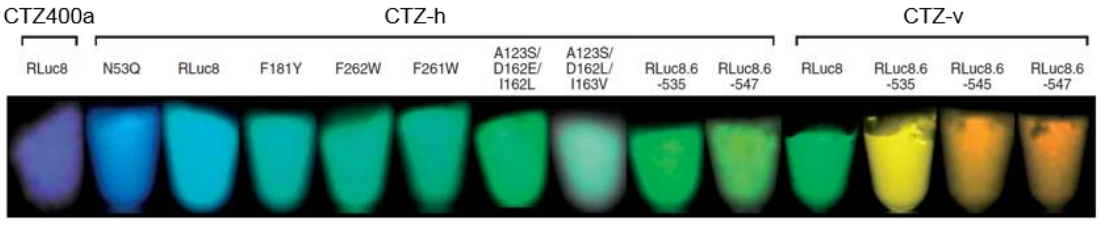

Figure 1. Bioluminescence of Rluc variants in the presence of coelenterazine 400a, native coelenterazine (Ctz-h) and coelenterazine v (Loening et al., 2007).

Thanks to the optimization of the various luciferases and substrates, the BRET mechanism can now be used efficiently in optogenetic. Recently, Tung et al. bypassed the use of an external light source to activate the inhibitory opsin eNpHR3.0. They coupled NpHR to a bioluminescent light source, a luciferase, exploiting the BRET mechanism. The resulting construct was named *ILMO2*[51] **[Figure 2A].** ILMO2 is a fusion protein composed of eNpHR3.0 and a construct called "Nanolantern", which is composed of a variant of RLuc, Rluc8 (S257G) fused to a variant of YFP, Venus **[Figure 2B]**. The function of Nanolantern is based on the BRET mechanism[52]. To optimize the BRET efficiency and the brightness of Nanolantern, Saito et al. constructed a protein chimera composed of a Venus protein truncated at the C terminal of 10 amino acids, and an Rluc8-S257G truncated at N terminal of 3 amino acids, linked by 3 amino acids. Rluc8(S257G) is activated by reaction with its specific substrate, coelenterazine h, with an emission spectrum at ~ 480 nm. ILMO2 was later shown to be functional to treat pathological conditions. It is able to suppress seizure activity after the focal injection of bicuculline methiodide in the hippocampus of anesthetized rats. Moreover, ILMO2 is most likely able to achieve a higher degree of suppression compared to the fiber-based illumination method because a larger volume of tissue is influenced, which is determined by the extent of iLMO2 expression rather than by light transmittance of an optical fiber[59].

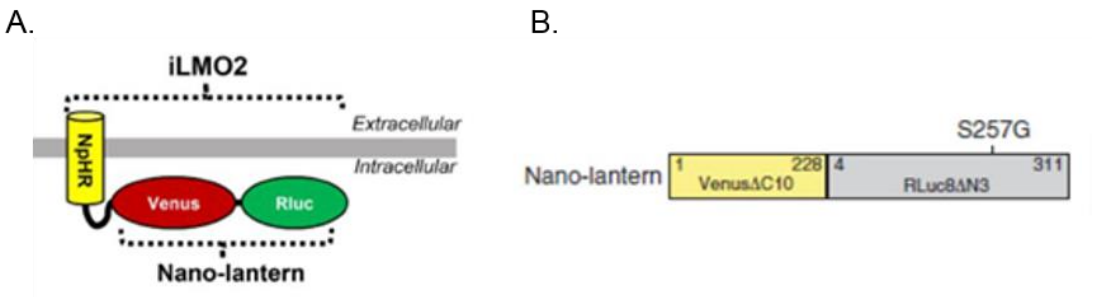

Figure 2. Schematic representation of the ILMO2 fusion protein (A)[51]and of the Nanolantern fusion protein (B)[52].

2. Aim of the thesis

The purpose of this work is to develop a new strategy to reduce neuronal hyperexcitability, with the aim of devising novel therapeutic approaches to ameliorate the epileptic phenotype. To this aim, we engineered a new probe, pHIL, which takes advantage of chemogenetics, optogenetics and of the intracellular acidification that occurs during epileptic conditions to reduce the neuronal hyperexcitability state. pHIL is composed of eNpHR3.0, a chloride pump that inhibits neuronal firing when activated by green/yellow light, E2GFP, a ratiometric pH sensitive variant of GFP, and RLuc8(S257G), a mutant of Renilla luciferase whose emission is blue-shifted upon reaction with CTZ 400a, a specific coelenterazine variant. When the intracellular pH decreases, such as during epileptic conditions, and upon the addition of CTZ 400a, the probe is activated. The light cascade starts with the emission of near-UV light (≈ 405 nm) from RLuc8(S257G). This light will activate E2GFP selectively under acidic conditions. E2GFP will in turn emit 510 nm light that will activate NpHR3.0, ultimately inhibiting neuronal firing.

- Our first aim was to engineer the active and control probes through molecular cloning. Five different constructs were cloned, two for the characterization of the probe in HEK293T cells and three for AAV2.9 production and the subsequent characterization of the probe in primary neurons and in vivo.
- We then studied the expression and localization of the probes in HEK293T cells using immunofluorescence and western blot techniques, and characterized the light cascade taking advantage of the BRET in vitro detection assay. We also characterized the function of the probe using patch clamp recordings, analyzing the changing in HEK293T membrane potential upon addition of CTZ400 a.

- Finally, we started the characterization of pHIL in primary hippocampal neurons analyzing its localization and expression. In parallel, we studied neuronal intracellular acidification in an in vitro model of epilepsy through live cell imaging. We also performed functional studies on pHIL expressing neurons taking advantage of cell-attached patch clamp recordings.

3. Materials and methods

3.1 Cloning strategies

a. pHIL and control plasmids

All restriction enzymes were from Promega (Madison, Wisconsin) unless otherwise indicated; all the final plasmids were verified by direct sequencing. All constructs were initially cloned in the pcDNA3.1 plasmid under the control of the cytomegalovirus (CMV) promoter. The eNpHR3.0 and the ΔN3-RLUC8-S257G sequences were amplified from the plenti-ILMO2 and pAAV2-ILMO2 constructs (a gift of Dr. Gross, Emory University, Atlanta, Georgia, USA), respectively. The truncated form of E^2GFP (ΔN12-E^2GFP-ΔC15) was amplified from pcDNA-E^2GFP (a gift of Dr. Bizzarri, NEST CNR-INFM, Scuola Normale Superiore, Pisa, Italy).

- To obtain the Ctrl construct, the ΔN3-RLUC8-S257G sequence was PCR amplified using the Pfu DNA Polymerase (BiotechRabbit, Berlin, Germany #BR0300101) and the following primers:

  Fw: 5'-ATCCggtaccaaggtgtacgaccccgag-3'

  Rv: 5'-ATCCgaattcttacacctcgttctcgtagc-3'

  Both pcDNA3.1 and ΔN3-RLUC8-S257G were subsequently digested with the ECORI/KPNI restriction enzymes and ligated using T4 ligase.

  The ΔN12-E^2GFP-ΔC15 sequence was PCR amplified using the Pfu DNA polymerase and the following primers:

  Fw: 5'-ATCCaagcttagggatccatggtgagcaagggcgaggagctg-3'

  Rv: 5'- ATCCggtaccccggcggcggtcacgaac-3'

  Both ΔN12-E^2GFP-ΔC15 and pcDNA-ΔN3-RLUC8-S257G were digested with the HINDIII/KPNI restriction enzymes and then ligated to insert ΔN12-E^2GFP-ΔC15 upstream of ΔN3-RLUC8-S257G (**Figure 3**).

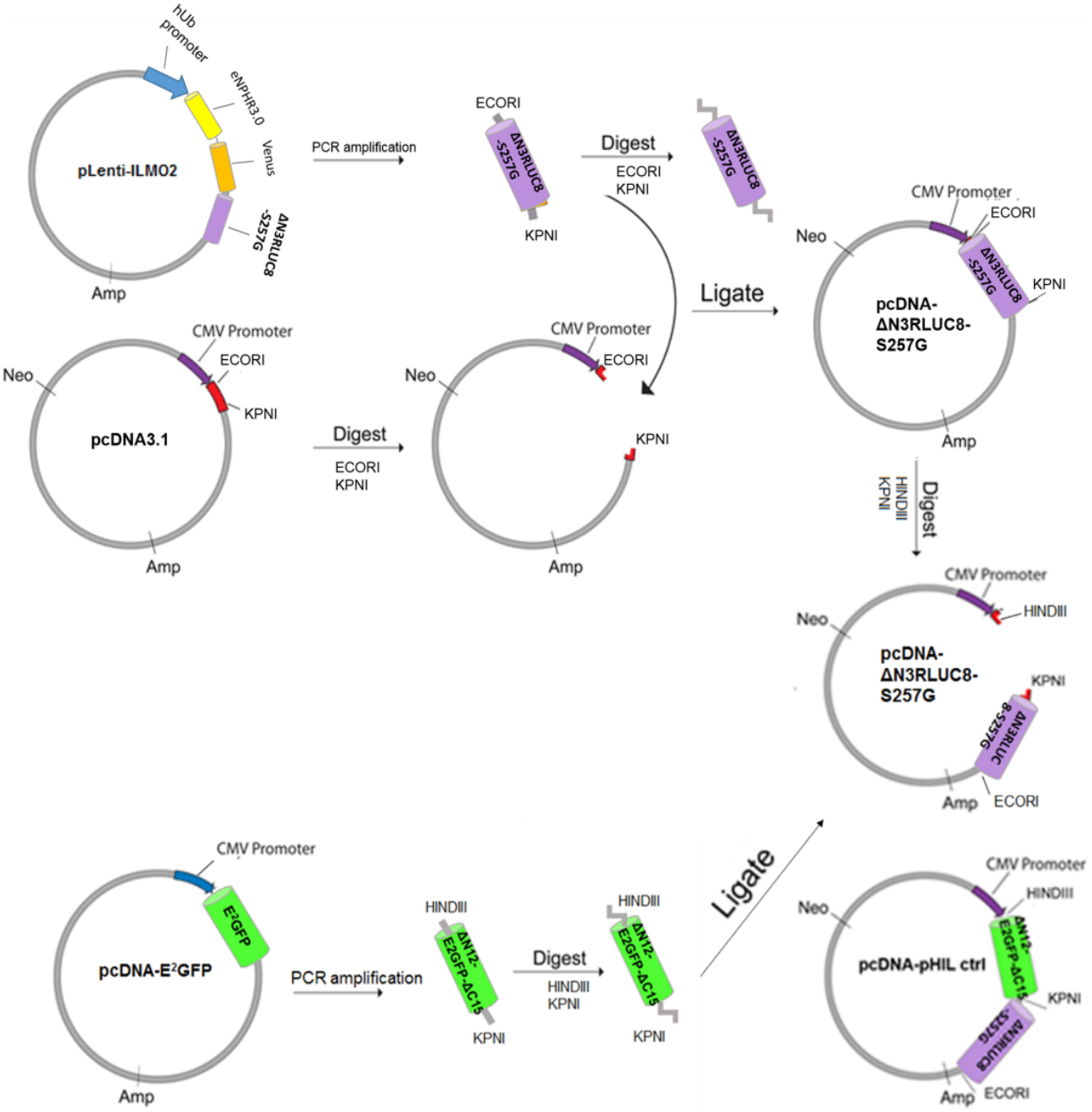

Figure 3. Schematic representation of the cloning strategy used to engineer the ctrl construct.

- To obtain the pHIL construct, eNpHR3.0 was PCR amplified using the Pfu DNA polymerase and the following primers:

  Fw: 5'-ATCCggatccatgacagagaccctgcctcccG-3'

  Rv: 5'-ATCCgcggccgcatcatcagccggggtc-3'

  Both pcDNA3.1 and eNpHR3.0 were subsequently digested with the BAMHI/NOTI restriction enzymes and ligated using T4 ligase.

  The ΔN12-E^2GFP-ΔC15 – ΔN3-RLUC8-S257G sequence was PCR amplified from the Ctrl plasmid using the Pfu DNA polymerase and the following primers:

  Fw: 5'- ATCCgcggccgcaGTGAGCAAGGGCGAGGAGCTG-3'

  Rv: 5'-ATCC CTCGAG gaattcttacacctcgttctcgtagc-3'

  Both pcDNA-eNpHR3.0 and the ΔN12-E^2GFP-ΔC15 – ΔN3-RLUC8-S257G sequence were digested with the NOTI/XHOI restriction enzymes and ligated, to insert the ΔN12-E^2GFP-ΔC15 – ΔN3-RLUC8-S257G sequence downstream of eNpHR3.0 (**Figure 4**).

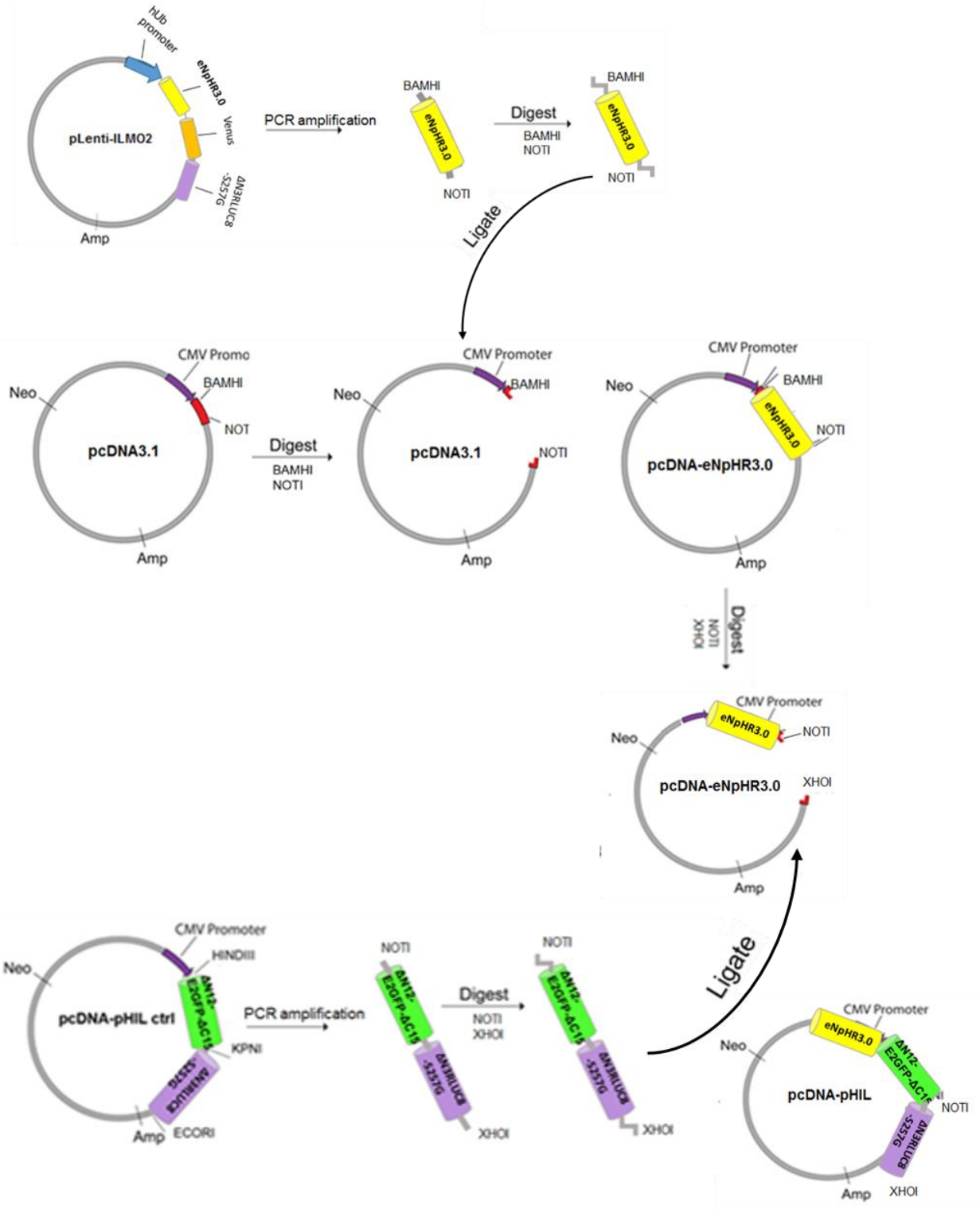

Figure 4. Schematic representation of the cloning strategy used to engineer the pHIL construct.

Both constructs also included an ER-export sequence (from pLenti-ILMO2) at the 3′ end of the fusion protein. The ER export sequence is a sorting signal that facilitates the ER export of proteins and their insertion in plasma membrane (Gradinaru et al.,2014).

The pHIL and Ctrl cassettes were subsequently cloned into the pAAV2 backbone (from pAAV2-ILMO2) for production of AAV2/9-pHIL and AAV2/9-ctrl. To achieve this, the pAAV2 backbone (pAAV2-ILMO2) , pcDNA-pHIL and pcDNA- Ctrl plasmids were digested with BAMHI/ECORI restriction enzymes and then ligated. To reduce the total plasmid length, in order to allow the production of AAV particles, the CaMKIIα (1.3 Kb) promoter was substituted with the CaMKIIα mini (0.3 Kb) promoter.

For the cloning of pAAV2- pHIL , the CaMKIIα mini (0.3 Kb) promoter was amplified from the pAAV2- ILMO2 plasmid using the Pfu DNA polymerase and the following primers:

Fw: 5'ATCCacgcgtacttgtggactaagtttgtt-3'

Rv: 5'-ATCCggatccgctgcccccagaactagggg-3'

Both CaMKIIα mini (0.3 Kb) promoter and the recipient vector (pAAV2-pHIL) were digested with the MLUI/BAMHI restriction enzymes and then ligated (**Figure 5B**).

For the cloning of pAAV2-ctrl , the CaMKIIα mini (0.3 Kb) promoter and the ΔN12-E^2GFP-ΔC15 – ΔN3-RLUC8-S257G sequence were PCR amplified from the pAAV2-pHIL ctrl (containing the CaMKIIα (1.3 Kb) promoter) using the Pfu DNA polymerase and the following primers:

Fw: 5'ATCCacgcgtacttgtggactaagtttgtt-3'

Rv: 5'-ATCCgaattcttacacctcgttctcgtagc-3'

Both CaMKIIα mini (0.3 Kb) - ΔN12-E^{2}GFP-ΔC15 – ΔN3-RLUC8-S257G sequence and the recipient vector (pAAV2-ctrl) were digested with the MLUI/ECORI restriction enzymes and then ligated (**Figure 5A**).

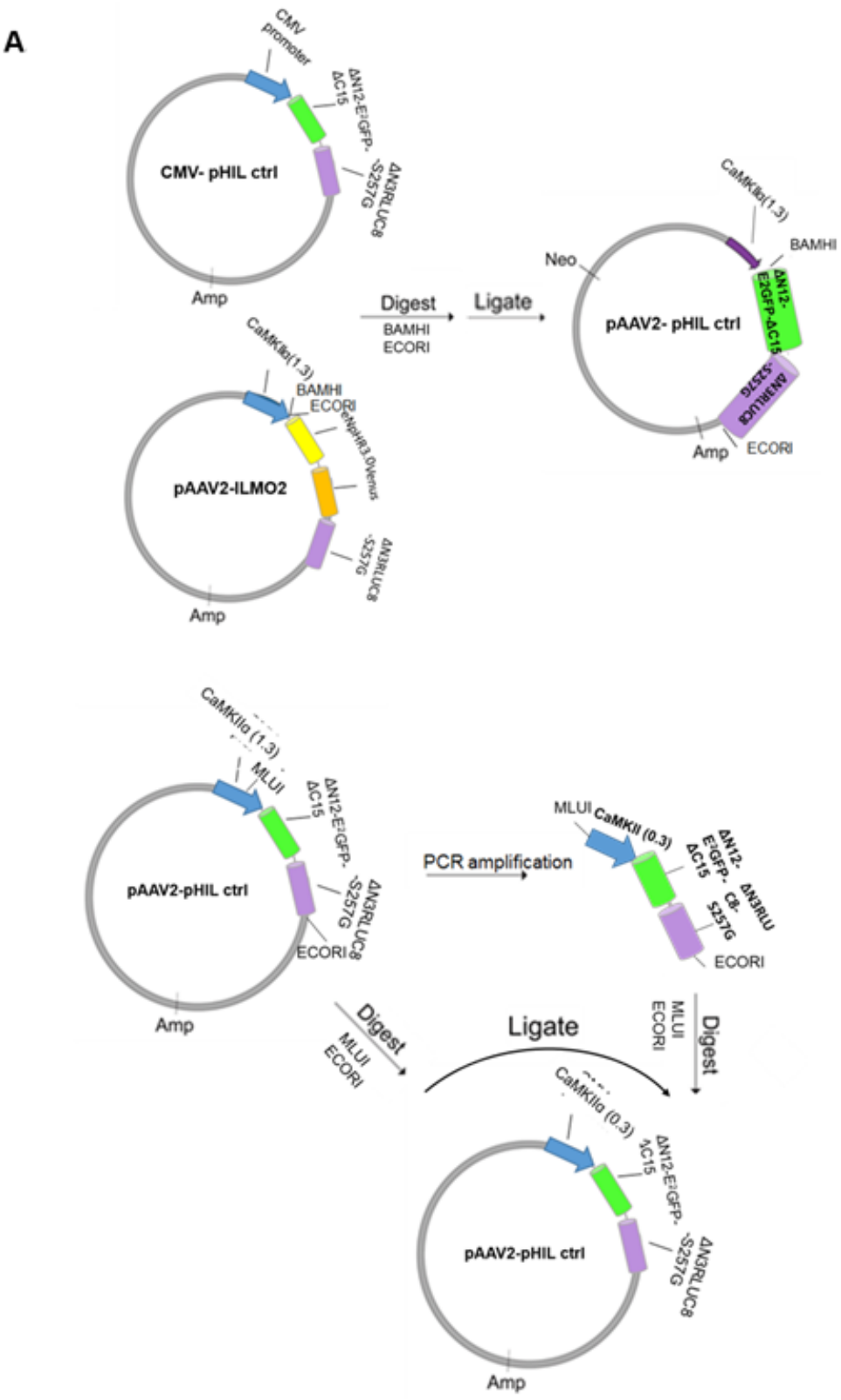

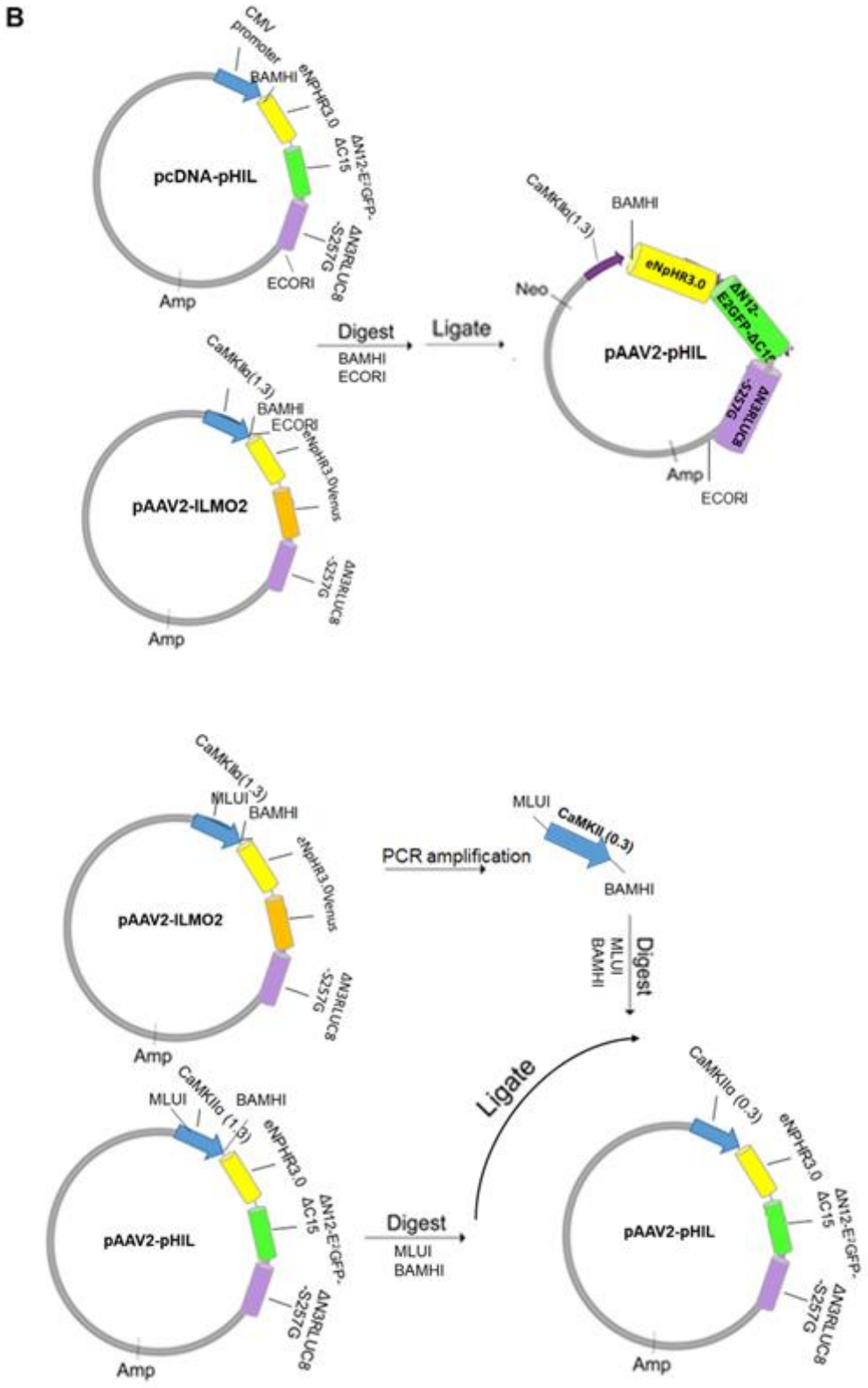

Figure 5. Schematic representation of the cloning strategy used to engineer the AAV2-pHIL (B) and the AAV2- ctrl (A) constructs with the mini CaMKIIα (0,3 Kb) promoter.

b. CD4 – ΔN12-E^{2}GFP-ΔC15

The truncated form of the E^{2}GFP (ΔN12 E^{2}GFP-ΔC15) was cloned in the hCD4-mOrange plasmid (#110192, Addgene, Watertown, Massachusetts, USA) downstream of the CD4 sequence. First, an ER export sequence was inserted downstream of truncated E^{2}GFP by PCR amplification using the following primers:

Fw: 5'-ATCCaagcttatggtgagcaagggcgaggagctg-3'

Rv: 5'-ATCCgtagcagaacccggcggcggtcac-3'

For the second PCR amplification, the ΔN12 E^{2}GFP-ΔC15/ER was used as template for a second PCR reaction using the following primers:

Fw: 5'-ATCCaagcttatggtgagcaagggcgaggagctg-3'

Rv: 5'-ATCCgaattcttacacctcgttctcgtagcagaa-3'

The amplified sequence and the hCD4-mOrange plasmid were digested with the HINDIII/ECORI restriction enzymes and then ligated [**Figure 6A**].

The CD4-ΔN12 E^{2}GFP-ΔC15/ER sequence was subsequently cloned in the lentiviral backbone plenti-Ub-iLMO2 (a gift of Dr. Gross), downstream of the ubiquitous promoter of human ubiquitin (hUb). CD4-ΔN12-E^{2}GFP-ΔC15/ER was PCR amplified using the following primers:

Fw: 5'-ATCCggatccatgaaccggggagtccc-3'

Rv: 5'-ATCCGaattcttacacctcgttctcgtagcagaa-3'

Both plenti-Ub-iLMO2 and the amplified sequence were digested with the BAMHI/ECORI restriction enzymes and ligated [**Figure 6B**].

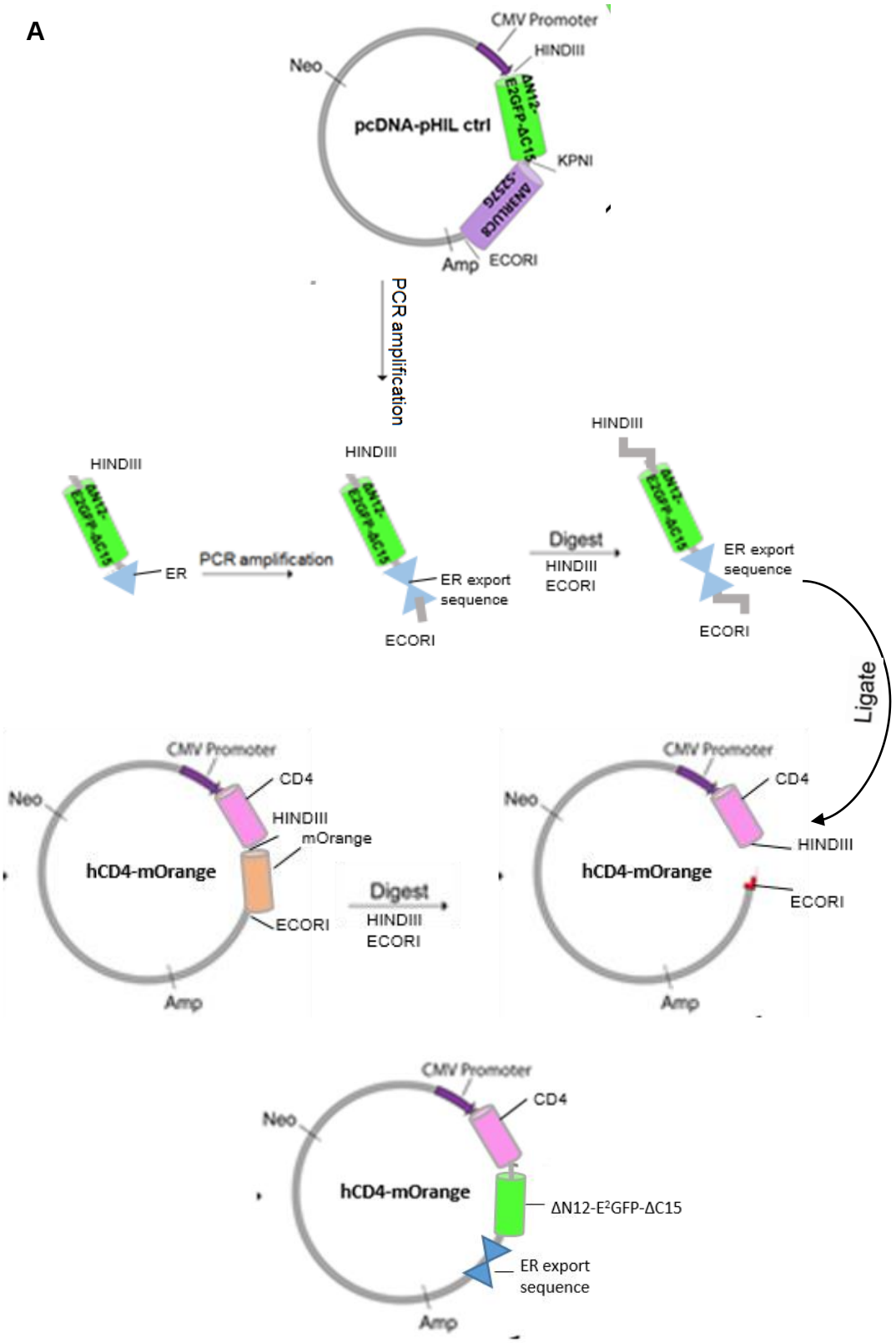
A
CMV Promoter
HINDIII
Neo
pcDNA-pHIL ctrl
ΔN12-E2GFP-ΔC15
KPNI
ΔNHIUCB
Amp
ECORI
PCR amplification
HINDIII
ΔN12-E2GFP-ΔC15
ER
PCR amplification
HINDIII
ΔN12-E2GFP-ΔC15
ER export sequence
ECORI
Digest
HINDIII
ECORI
HINDIII
ΔN12-E2GFP-ΔC15
ER export sequence
ECORI
Ligate
CMV Promoter
Neo
CD4
HINDIII
mOrange
hCD4-mOrange
ECORI
Amp
Digest
HINDIII
ECORI
CMV Promoter
Neo
CD4
HINDIII
hCD4-mOrange
ECORI
Amp
CMV Promoter
Neo
CD4
hCD4-mOrange
ΔN12-E²GFP-ΔC15
ER export sequence
Amp

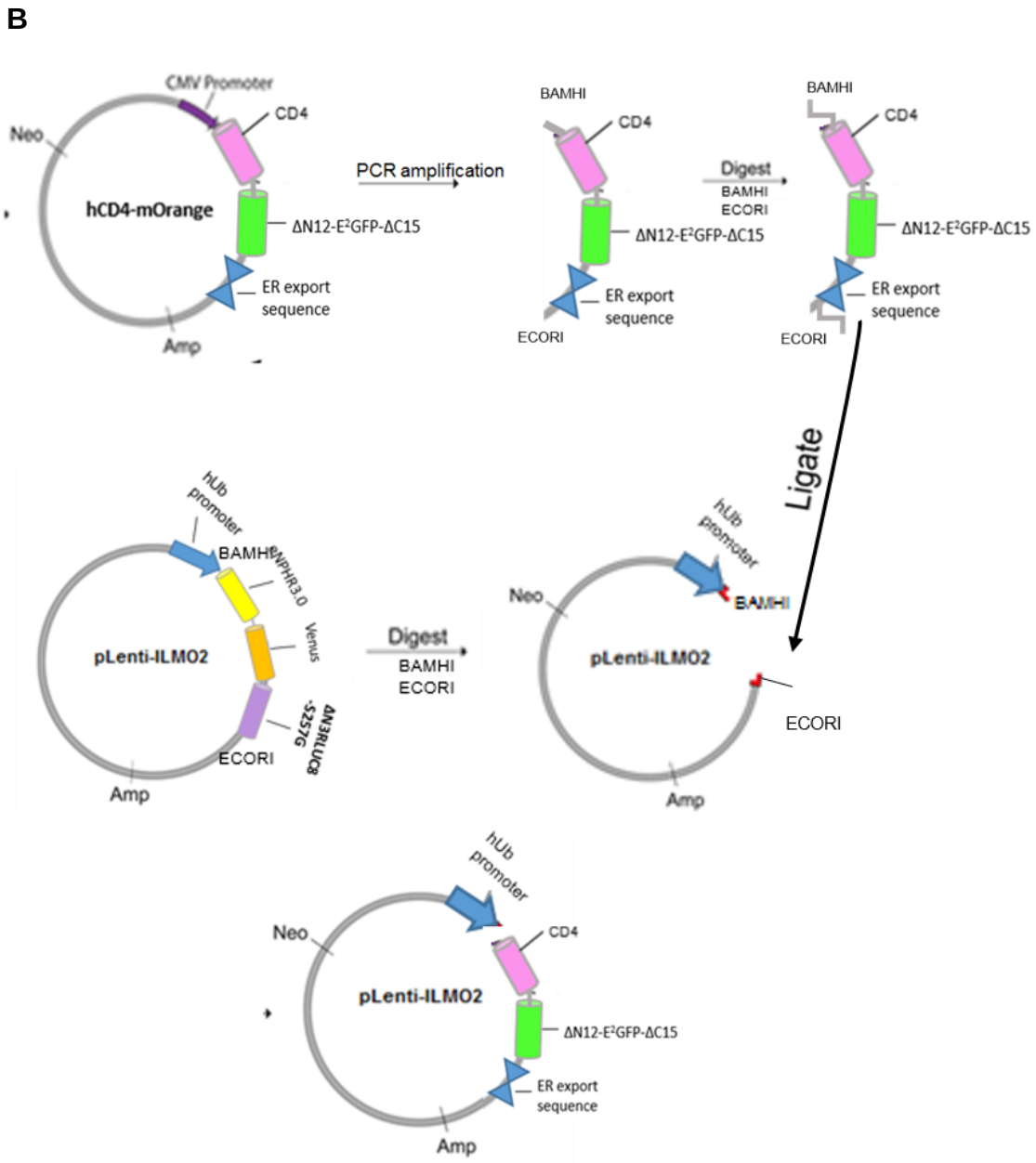

Figure 6. Schematic representation of the cloning strategy used to engineer the pLenti-hCD4-ΔN12 E^2GFP-ΔC15 construct.

After the cloning, the correct expected length of each construct was analyzed through renstriction enzymes digestion. Digestion products were, then, analyzed using agarose electrophoresis (1% agarose gel).

3.2 Cell cultures, transfection and infection

All cell culture reagents were from Invitrogen (Carlsbad, California,), unless otherwise specified.

Human embryonic kidney (HEK) 293 cells were cultured in Dulbecco's Modified Eagle Medium (DMEM) (Invitrogen #11995-073) supplemented with 10% fetal bovine serum (FBS), 1% glutamine and 1% Penicillin/Streptomycin (complete DMEM), in a humidified 5% CO_2 atmosphere at 37 °C. For splitting, cells were carefully washed with PBS and incubated with trypsin/EDTA for 1-2 min. Cells were subsequently centrifuged at 1000 rpm for 5 min, and then resuspended in fresh medium.

Hippocampal neurons were obtained from embryonic day (E)18.5 C57BL6/J mouse embryos. Hippocampi were dissected in ice-cold PBS, incubated with trypsin 0.125% for 15 min at 37 °C, and mechanically dissociated. Neurons were then resuspended and plated on poly-D-lysine-coated glass coverslips or plastic wells in Neurobasal medium containing 10% Fetal Bovine Serum (FBS), 1% glutamax and 1% Penicillin/Streptomycin. After 3 h, the medium was removed and replaced with neurobasal containing 2% B27 supplement, 1% glutamax (a dipeptide, L-alanine-L-glutamine, which is more stable in aqueous solutions) and 1% Penicillin/Streptomycin.

HEK293 cells and hippocampal primary neurons were transfected with using Lipofectamine 2000 following manufacturer's recommended protocols.

Hippocampal neurons were infected at DIV 3 with AAV2/9 CaMKIIα(0.3)-pHIL and with AAV2/9 CaMKIIα(0.3)-Ctrl following standard procedures (viruses were produced by TIGEM AAV vector core facility at a title of 10^{12} GC/ml). Experiments were performed at DIV14.

3.3 Immunofluorescence staining and confocal analysis

HEK293T cells and hippocampal neurons were plated on poly-D-lysine-coated 18 mm coverslips. 48 h after HEK293T cell transfection, cells were incubated with CellMask deep red (#C10046, Termofisher Scientific, Waltham, MA USA) an amphipathic molecule formed by a lipophilic moiety for membrane loading and a negatively charged hydrophilic dye to anchor the probe in plasma membrane. HEK293T cells were incubated with the probe for 5 minutes, washed with PBS 1x and analyzed for plasma membrane staining in live imaging using the Leica SP8 confocal microscope.

7 days after hippocampal neurons infection, samples fixed with PBS / 4% paraformaldehyde for 20 min and subsequently permeabilized for 5 min with PBS / 0.2% Triton X-100 and then incubated in blocking buffer (PBS / Tween 0.05% / 3% BSA) for 30 min. Cells were then incubated for 1 h at RT with primary antibodies (rabbit polyclonal anti-GFP, #A111222 Life Technologies, 1:200) diluted in blocking buffer, carefully washed and incubated for 45 min RT with secondary antibodies (Alexa Fluor® 488 anti rabbit, # A32790 Life Technologies, 1:500) diluted in blocking buffer. Coverslips were then mounted using ProLong antifade (#P36931, Life Technologies) and imaged using a Leica SP8 confocal microscope (Leica Mycrosistems, Wetzlar, Germany) with a 63X oil-immersion objective.

3.4 Protein extraction and western blotting

HEK293T cells and hippocampal neurons were lysed using RIPA buffer [0.5 mM EDTA, 20 mM Tris HCl pH 8, 100 mM NaCl, 0.5 % Np40, 0.5% Na-deoxycholate, protease inhibitor cocktail (#04693116001, Roche Applied Science, Penzberg, Germany), phosphatase inhibitor cocktail 2 (#P5726, Sigma, St. Louis, Missouri, USA) and phosphatase inhibitor cocktail 3 (#P0044, Sigma)]. The final

protein concentration was quantified using the BCA protein assay kit (#23225, Pierce Biotech, Waltham, Massachusetts, USA).

Proteins were separated on the basis of their molecular weight through sodium dodecyl sulfate- polyacrylamide gel electrophoresis (SDS-PAGE) and subsequently transferred to a nitrocellulose membrane, following standard protocols. Membranes were incubated in blocking buffer (1X TBST / 5% w/v nonfat dry milk) for 1 h and then incubated with primary antibodies diluted in blocking buffer for 1 h (antibodies used are summarized in the **Table 1**.). Membranes were then washed several times in TBST incubated with secondary antibodies (goat anti-rabbit IgG (H+L), Peroxidase Conjugated, #PR31460, Life technologies) for 45 min and revealed using ECL™ Blotting Reagents (#RPN2109, GE Healthcare, Chicago, Illinois, USA).

Antibody	Source	Cat.Number	Diluition	Company
GFP	Rabbit	A111222	1:1000	Life Technologies (Carlsbad, USA)
Renilla Luciferase	Rabbit	ab185926	1:1000	Abcam (Cambridge,UK)
α- Actin	Rabbit	A2066	1:5000	Sigma-Aldritch (St.Louis, USA)
GAPDH	Rabbit	14C10	1:10000	Cell Signaling (Danvers, USA)

Table 1. Primary antibodies used for western blot analysis.

3.5 Coelenterazine preparation

Coelenterazine 400a (CTZ 400a) was purchased from Santa Cruz Biotechnology (Dallas, Texas, USA) (#sc-280647) and solubilized in Ethanol 100% at 1 mM following manufacturer's recommended protocol. Before every experiment,

the stock solution was diluted in 20 mM (2-Hydroxypropyl)-β-cyclodextrin (Sigma, #H5784) to the required concentration (5, 10, 20, 40, 50 µM) and added to the external recording solution. Coelenterazine-h (CTZ h) (Promega, #S2011) was solubilized in 20 mM (2-Hydroxypropyl)-β-cyclodextrin in PBS as described by Dr Osamu Shimomura[57] and used at the final concentration of 20 µM[51]. Frozen stock solutions were kept at -20°C and protected from light.

3.6 Bioluminescence Resonance Energy Transfer (BRET) in vitro detection assay.

HEK293T cells were plated in a six well plate at a concentration of 250,000 cells/well. After 24 h cells were transfected with pHIL, control plasmid, or with a construct coding RLUC8-S257G as a negative control (pTRE-Tight-RLuc8-S257G, Addgene, #79844). The day after transfection, cells were trypsinized, resuspended and plated in a 96 well plate (96 Well White Polystyrene Microplate, #CLS3610, Corning®, Corning, New York, USA) in complete DMEM w/o phenol red (#31053028, Life Technologies) and w/o Penicillin/Streptomycin at a concentration of 75,000 cell/well. The experiment was performed adding CTZ 400a at increasing concentrations (10, 20, 50 µM); the luminescence intensity and the fluorescence of RLUC8-S257G and E^2GFP were detected using the TECAN 500F machine in the Luminescence Dual Color mode (magenta/green filters) under three different pHi conditions. Buffers used to change the intracellular pH were composed as follows: pH 6 buffer: 1mM $MgCl_2$, 10 mM MES, 100 mM KCl, 100 mM NaCl, 1.36 mM $CaCl_2$, 10 mM glucose, 20 µM nigericin; pH 7.4 and pH 8 buffers: 1mM $MgCl_2$, 10 mM HEPES, 100 mM KCl, 100 mM NaCl, 1.36 mM, $CaCl_2$, 10 mM glucose, 20 µM nigericin. All experiments were performed at RT in the dark.

The BRET ratio was calculated as follows: (I510 / I405)HALO-E2GFP-RLUC8 - (I510 / I405)RLUC8 [60].

3.7 Time Lapse Live Cell imaging

Hippocampal neurons were plated on poly-D-lysine-coated 25 mm coverslips, transfected with pLenti-CD4/ΔN12 E^2GFP-ΔC15 and imaged at 10 DIV. Live cell imaging was performed using a Leica SP8 laser scanning confocal microscope equipped with a 40x oil immersion objective. The sequential excitation of E^2GFP at 405 nm and 488 nm was achieved with a multiline argon laser. Emitted fluorescence was collected between 510 nm and 560 nm using a single photomultiplier tube (PMT) at a constant voltage. Before every experiment, coverslips with cells were positioned in a chamber and a pH calibration curve was performed by adding in the chamber, initially, a K^+ enriched buffer composed as follows: 120 mM potassium gluconate, 40 mM NaCl, 20 mM HEPES, 0.5 mM $CaCl_2$, 0.5 mM $MgSO_4$ pH 7.5. Cells were subsequently perfused with the same buffer, adjusted to the desired pH by adding HEPES for pH>7, NaOH and MES for pH <7, and supplemented with nigericin 10 µM and valinomycin 10 µM. The calibration curve was performed at pH 5.5, 6, 6.5, 7, 7.5. Images were taken 10 min after the addition of the buffer supplemented with ionophores (Bizzarri et al.,2006).

To determine the intracellular pH value during epileptic-like conditions, cells were first perfused with a buffer composed as follows: 140 mM NaCl, 2.5 mM KCl, 1.8 mM $CaCl_2$, 1 mM $MgCl_2$, 20 mM HEPES, 10 mM glucose, pH 7.4. The fluorescence was collected for 2 min to obtain the baseline, after which 30 µM bicuculline (#0131, TOCRIS, Bristol, UK) was added and fluorescence was collected for additional 8 min. Confocal images were analyzed using the Image J software.

First, regions of interest (ROIs) were chosen for each image. The area of each ROI was about 2 μm^2, positioned on discrete structures visible on neurite extensions. Fluorescence intensity ratios were calculated according to the equation $R = MV_{405} / MV_{488}$, where MV_{405} (mean value) is the average pixel intensity for each ROI when ΔN12-E^{2}GFP-ΔC15 is excited with 405 nm light, while MV_{488} is the average pixel intensity for each ROI when ΔN12-E^{2}GFP-ΔC15 is excited with 488 nm light (Chiacchiaretta et al., 2017).

$$R = \frac{MV(\lambda_x 405 - \lambda_e 510 - 560) - MV\,(background)}{MV(\lambda_x 488 - \lambda_e 510 - 560) - MV\,(background)}$$

Emission fluorescence ratios were converted to pH values according to the calibration curves collected by fitting each ratio value in a sigmoidal dose response curve using the Graphpad Prism 7.04 software.

3.8 Intracellular Recordings

Intracellular recordings were performed on HEK293T cells transfected with CMV-pHIL and control plasmids, plated on petri dishes. For all the experiments, cells were maintained in extracellular standard solution (Tyrode) containing: NaCl 140 mM, KCl 4 mM, $CaCl_2$ 2 mM, $MgCl_2$ 1 mM, HEPES 10 mM, Glucose 10 mM, pH 7.3 with NaOH. Current-clamp recordings were performed at a holding potential of 0 mV. The intracellular pH was changed through the patch pipette using an internal solution at three different pH: 6, 7.4 and 8. The internal solution was composed by: K^+ gluconate 126 mM, NaCl 4 mM, $MgSO_4$ 1 mM, $CaCl_2$ 0.02 mM, Bapta 0.1 mM, Glucose 15 mM, HEPES 5 mM, ATP 3 mM, GTP 0.1 mM. For the acidic solution (pH 6) HEPES was substituted with MES 5 mM. CTZ 400a and CTZh were added directly to the external solution, during the recording, at a final concentration of respectively 10 µM and 40 µM. All experiments were performed at RT in the dark.

Data acquisition was performed using PatchMaster program (HEKA Elektronic, Lambrecht/Pfalz, Germany).

Voltage-clamp cell-attached recordings were performed at a holding potential of -70 mV. Cells were recorded in continuous for 5 min without applying any currents in three different external solutions: (i) Tyrode, (ii) Tyrode with bicuculline (30 µM) and (iii) Tyrode with bicuculline (30 µM) and CTZ400a (40 µM). Action potentials spikes were analyzed with Clampfit (AxonTM pCLAMPTM) spikes and bursts detector.

4. Results

4.1 Molecular Cloning of pHIL and control probes

a. Engineering of pcDNA-pHIL and pcDNA-ctrl

To obtain a probe able to reduce neuronal hyperexcitability, we coupled a bioluminescent protein with an inhibitory opsin and with a pH sensor to control neuronal hyperexcitability upon intracellular acidification, a phenomenon observed during epileptic conditions (Ahmed and Connor, 1980; Xiong et al., 2000). The resulting chimeric protein was named pHIL, for pH-sensitive Inhibitory Luminopsin. pHIL is composed of the enhanced version of Natromonas Pharaonis Halorhodopsin (eNpHR3.0) (Gradinaru et al., 2010) the pH-sensitive variant of GFP, E2GFP (Bizzarri et al., 2006) truncated at the N terminal and C terminal of 12 and 15 amino acids respectively (ΔN12-E2GFP-ΔC15), and the mutated Renilla Luciferase truncated at the N terminal of 3 amino acids (ΔN3-RLUC8-S257G, Saito et al., 2012). Proteins were truncated in order to decrease the space between them, thus facilitating the transfer of energy. ΔN12-E2GFP-ΔC15 and ΔN3-RLUC8-S257G are linked by two amino acids (Gly and Thr), while ΔN12-E2GFP-ΔC15 is linked to eNpHR3.0 by three alanines51,52. The sequences coding eNpHR3.0-ΔN12-E2GFP-ΔC15-ΔN3-RLUC-8S257G (pHIL) and the control construct ΔN12-E2GFP-ΔC15-ΔN3-RLUC8-S257G (ctrl) were cloned in pcDNA3.0 under the control of the cytomegalovirus promoter (CMV).

The expected lengths of plasmids obtained from the cloning are 7978 bp for pHIL and 7116 bp for the control. To confirm that the cloning was successful,, a restriction enzyme digestion was performed. pcDNA-ctrl was digested with BAMHI, EAGI and SALI restriction enzymes obtaining bands of: 7116 bp (BAMHI), 1269 bp and 5847 bp (EAGI), 2188 bp and 4928 bp (SALI) [Figure 7A]. pcDNA-pHIL was

digested with XBAI, EAGI, and SALI restriction enzymes obtaining bands of: 7978 bp (XBAI), 2915 bp and 5063 bp (EAGI); 2188 bp and 5790 bp (SALI) [Figure 7B]. The results of plasmids digestions confirmed that the cloning was successful.

b. Engineering of pAAV2-pHIL and pAAV2- ctrl

In order to produce a tool suitable to be used both for in vitro experiments on primary neurons as well as for in vivo experiments, sequences coding pHIL and ctrl probes were cloned in an AAV2 vector under the control of the Ca2+/Calmodulin-dependent kinase IIα (CaMKIIα) promoter to have the expression only in excitatory neurons of the postnatal forebrain39. It is known that AAVs cargo capacity is between 4.1 and 4.9 kb61. In order to create a transgene that is short enough to be compatible with AAV limited packaging capacity, a truncated and shorter version of the CamKIIα promoter was used, which is about 0.3 Kb, compared to 1.3 Kb of the original promoter62 . This shorter sequence was inserted upstream of the pHIL and ctrl sequences in the AAV2 vector. The expected length of plasmids is 6943 bp for pHIL and 6078 bp for the control. To confirm that, the cloning was successful, a restriction enzyme digestion was performed. pAAV2-ctrl was digested with ECORI, KPNI, PVUII and NOTI restriction enzymes obtaining bands of: 6078 bp (ECORI), 699 bp and 5379 bp (KPNI), 2619 bp and 3459 bp (PVUII), 2887 bp and 3191 bp (NOTI) [Figure 7C]. pAAV2-pHIL was digested with ECORI, PVUII, and NOTI restriction enzymes obtaining bands of: 6943 bp (ECORI), 2619 bp and 4324 bp (PVUII), 2799 bp, 2887 bp and 1257 bp (NOTI) [Figure 7D]. The results of plasmids digestions confirmed that the cloning was successful.

c. Engineering of pLenti-CD4/E^{2}GFP

pHIL is activated only under acidic conditions. It is known that, during seizure activity, neurons accumulate H+, resulting in acidification of the intracellular space16. In order to study activity-induced intracellular acidification in primary hippocampal neurons, pLenti-CD4/E2GFP was constructed. ΔN12-E2GFP-ΔC15 was cloned downstream of the human cluster of differentiation 4 (CD4) receptor transmembrane sequence, to target the E2GFP to the intracellular side of the plasma membrane, under the control of the human ubiquitin promoter (hUb), in a lentiviral vector (pLenti). The expected length of plasmid obtained is 11280 bp. To confirm that the cloning was successful, a restriction enzymes digestion was performed. pLenti-CD4/E2GFP was digested with BAMHI, EAGI and SACII restriction enzymes obtaining bands of: 11280 bp (BAMHI), 7258 bp and 4022 bp (EAGI), 3834 bp and 7446 bp (SACII) [Figure 7E]. The results of plasmids digestions confirmed that the cloning was successful.

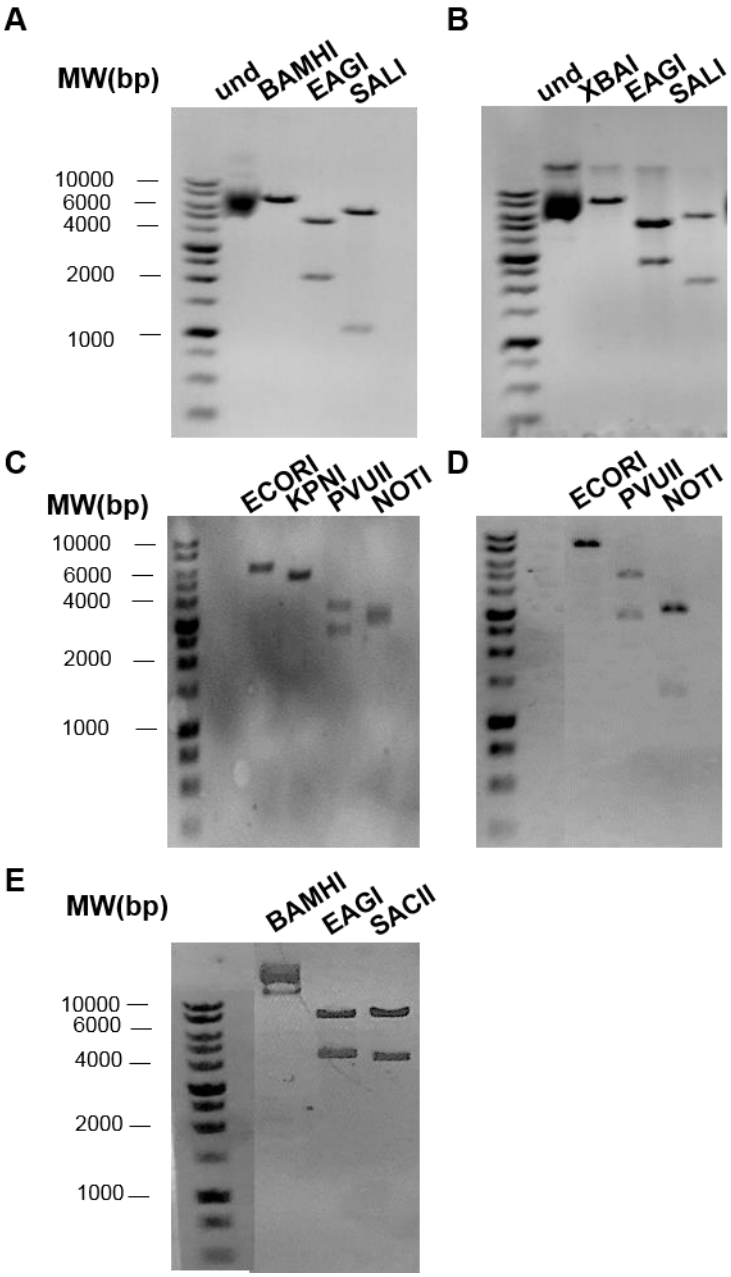

Figure 7. Cloning products restriction enzymes digestion. Agarose gels illustrating the products of pcDNA-pHIL (A), pcDNA-ctrl (B), pAAV2-pHIL (C), pAAV2-ctrl (D) and pLenti-CD4/E2GFP (E) digestions with various restriction enzymes. For details, see text.

4.2 Validation of pHIL and ctrl expression and localization in HEK293T cells.

HEK293T cells were transfected with the constructs (pcDNA-pHIL and pcDNA-ctrl) **[Figure 8A]** and their expression and localization was verified. Western blot analysis was performed by using antibodies against Rluc8. As shown in [**Figure 8B**], the fusion proteins show a molecular weight of 93 kDa and 62 kDa respectively, as expected. In order to verify the localization of the two probes, confocal live cell imaging was performed. HEK293T were transfected with the two constructs and subsequently treated with CellMask Deep Red (see material and methods) for plasma membrane staining. Colocalization of pHIL with the plasma membrane was observed [**Figure 8C** *upper panel*], while the ctrl construct was observed in the cytoplasm, as expected [**Figure 8C** *lower panel*].

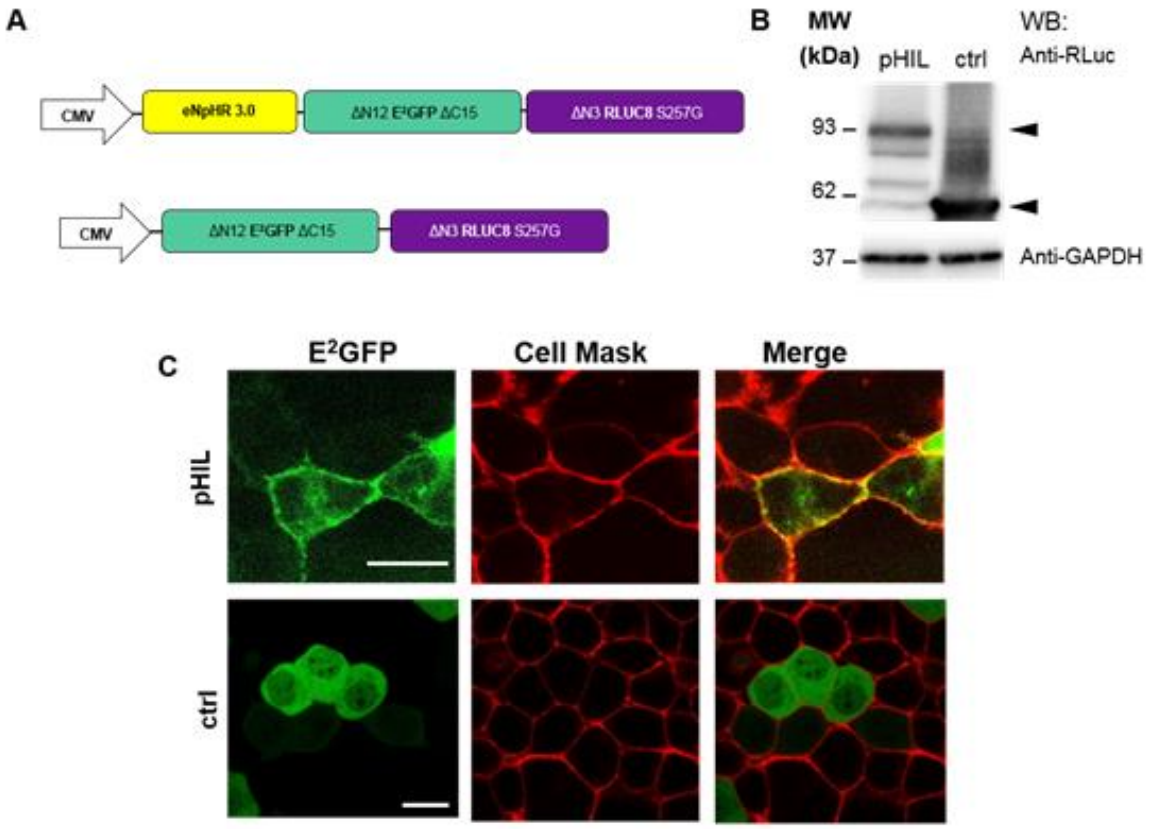

Figure 8. pHIL and control constructs structure, expression and localization in HEK293T cells. (A) Schematic illustration of pHIL and control constructs. For details, see text. Both fusion proteins were cloned into pcDNA3.0 under the control of the cytomegalovirus promoter (CMV). (B) Western blot showing pHIL and control expression (arrowheads) in HEK293T cells. The expression of the fusion proteins was analyzed using anti-RLuc antibodies. Anti-glyceraldehyde-3-phosphate dehydrogenase (GAPDH) antibodies were used to verify equal loading. (C) Representative confocal images showing membrane localization of pHIL (*upper panel)* and cytoplasmic localization of the control construct *(lower panel).* Cell Mask was used as a marker of plasma membrane (red channel). Scale bars: 20 µm for pHIL, 15 µm for the control.

4.3 Analysis of the light cascade steps leading to the activation of pHIL.

The activation of pHIL is based on a light cascade that culminates in the activation of eNpHR3.0. After the addition of coelenterazine 400a (CTZ 400a), ΔN3-RLUC8-S257G is activated and emits 405 nm light. UV light, under acidic conditions, activates the pH sensor ΔN12-E^{2}GFP-ΔC15 that emits 510 nm light (BRET). The light emitted by ΔN12-E^{2}GFP-ΔC15 in turns activates eNpHR3.0 (FRET) to hyperpolarize neurons [**Figure 9A**].

In order to better characterize the function of pHIL, every step of the light cascade, from the addition of CTZ 400a to the activation of eNpHR3.0, was analyzed. First the BRET efficiency was measured at acidic (pH 6) and alkaline pH (pH 8) with respect to the physiological condition (pH 7.4). HEK293T cells were transfected with pHIL or with a construct coding ΔN3-RLUC8-S257G only as a negative control; CTZ 400a was added at increasing concentrations and the intensity of the luminescence emitted by ΔN3-RLUC8-S257G (405 nm) and of the fluorescence emitted by ΔN12 E^{2}GFP ΔC15 (510 nm) was measured using the TECAN 500F machine. After this, the BRET ratio was calculated as follows: $(I_{510} / I_{405})_{HALO\text{-}E2GFP\text{-}RLUC8}$ - $(I_{510} / I_{405})_{RLUC8}$. As reported in [**Figure 9B**], BRET ratio values are higher at pH 6 than at pH 8 and pH 7.4 indicating that the energy transfer between ΔN3-RLUC8-S257G and ΔN12-E^{2}GFP-ΔC15 is higher under acidic conditions, consistent with the increased absorbance of E^{2}GFP in the acidic environment. To justify these results, we analyzed in detail every step of the light cascade starting with the analysis of the 405 nm light emitted by the ΔN3-RLUC8-S257G at pH 6 and at the control pH (7.4). The analysis was done in cells transfected with the ctrl construct in order to consider the BRET event first. In the graph is shown that the ΔN3-RLUC8-S257G

emission at pH 6 is lower with respect to control pH. This is because the light emitted is absorbed by the E^2GFP in the acidic environment **[Figure 9C].**

The second step of the light cascade is the FRET between ΔN12-E^2GFP-ΔC15 and eNpHR3.0. To analyze this step, E^2GFP total emission was measured in cells transfected with pHIL and ctrl plasmids setting the pH to 6 and 7.4 and adding increasing concentrations of CTZ400a. In the graph shown in [**Figure 9D**], is clear that, under acidic conditions, E^2GFP total emission is lower in cells transfected with pHIL with respect to cells transfected with the ctrl construct at pH 6. This is because the light emitted by E^2GFP is absorbed by eNpHR3.0 in the pHIL probe, and not absorbed in the ctrl probe. For the control pH, the E^2GFP total emission for the control construct is lower with respect to pH 6 because in neutral pH the E^2GFP will adsorb a smaller amount of light coming from the ΔN3-RLUC8-S257G. Finally, the E^2GFP total emission in cells transfected with pHIL is higher for the control pH with respect to the pH 6. This is because the light emitted by E^2GFP will be absorbed by the eNpHR3.0 but the amount of light is not enough to activate it (see paragraph 4.4).

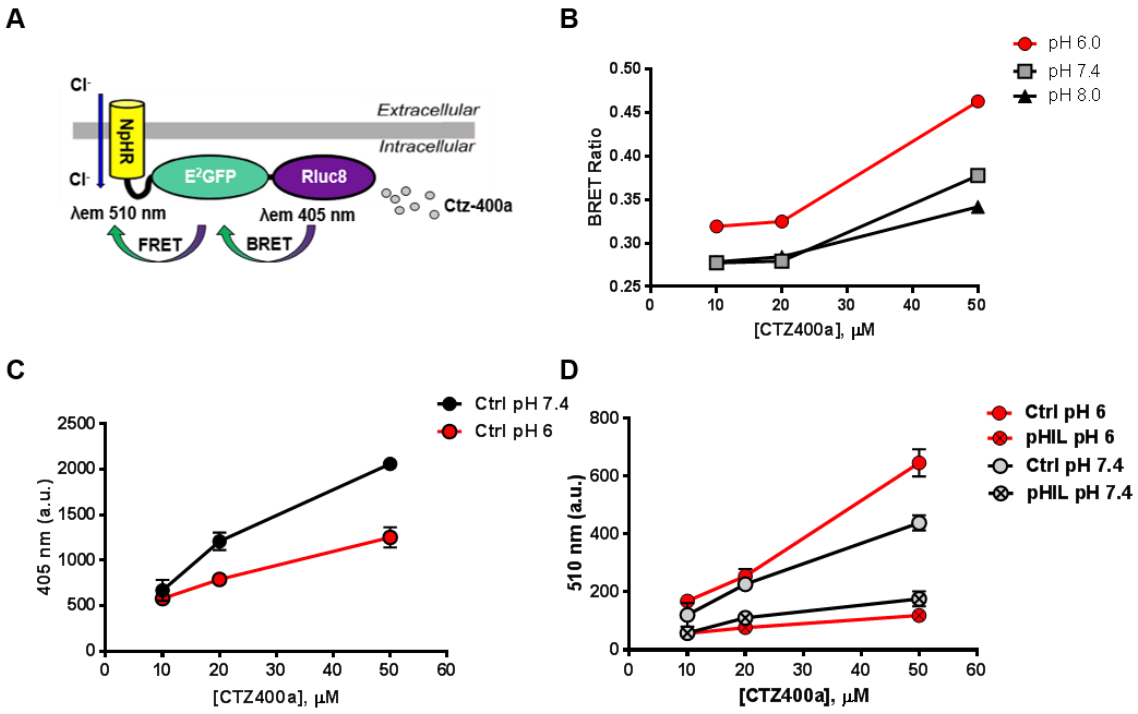

Figure 9. **Characterization of pHIL light cascade mechanism**. (A) Schematic illustration of pHIL functioning, showing: (i) the activation of ΔN3-RLUC8-S257G after the addition of CTZ400a and the consequent emission at 405 nm; (ii) under acidic conditions the light emitted by ΔN3-RLUC8-S257G activates ΔN12-E^{2}GFP-ΔC15 that will emit at 510 nm (BRET); (iii) the light emitted by ΔN12-E^{2}GFP-ΔC15 activates eNpHR3.0 (FRET). (B) Plot of BRET ratio from HEK293T cells transfected with pHIL after the addition of CTZ 400a (10, 20 and 50 µM) and under different pH conditions. Mean ± SEM, n=4 indipendent preparations, p>0,05 one-way ANOVA. (C) Plot of ΔN3-RLUC8-S257G emission from HEK293T cells transfected with ctrl constructs after the addition of CTZ 400a (10, 20 and 50 µM) at pH 6 and 7.4. Mean ± SEM, n=4 indipendent preparations, p>0,05 one-way ANOVA. (D) Plot of E^{2}GFP total emission from HEK293T cells transfected with pHIL and ctrl constructs after the addition of CTZ 400a (10, 20 and 50 µM) and at pH 6 and 7.4. Mean ± SEM, n=4 indipendent preparations, p>0,05 one-way ANOVA .

4.4 Electrophysiological characterization of pHIL in HEK293T cells.

In order to analyze if, after the addition of CTZ 400a, the light emitted by ΔN12-E^{2}GFP-ΔC15 under acidic conditions is able to activate eNpHR3.0, HEK293T cells were transfected with pHIL and ctrl constructs and electrophysiological recordings were performed upon addition of CTZ 400a (10 µM) and by changing intracellular pH through the patch pipette. Plasma membrane hyperpolarization was observed at acidic intracellular pH (pH 6), while no hyperpolarization was observed at physiological (pH 7.4) and alkaline (pH 8) pH in cells transfected with pHIL [**Figure 10A, 10B**]. In cells transfected with the control construct, no hyperpolarization was observed under any pH condition [**Figure 10C**]. In order to confirm that the activation of pHIL occurs only when ΔN12-E^{2}GFP-ΔC15 absorbs the 405 nm light coming from ΔN3-RLUC8-S257G, electrophysiological recordings were performed in HEK293T cells transfected with pHIL and ctrl probes by changing intracellular pH and upon addition of CTZ h (20 µM) , which causes ΔN3-RLUC8-S257G to emit at 488 nm, which should not activate ΔN12-E^{2}GFP-ΔC15 under acidic conditions. Accordingly, no hyperpolarization was observed in cells transfected with pHIL [**Figure 10D**] or the ctrl probe [**Figure 10E**] under any of the tested pH conditions. This is because ΔN3-RLUC8-S257G is too far to activate eNpHR3.0, and because ΔN12-E^{2}GFP-ΔC15 will emit only when illuminated with near-UV light.

.

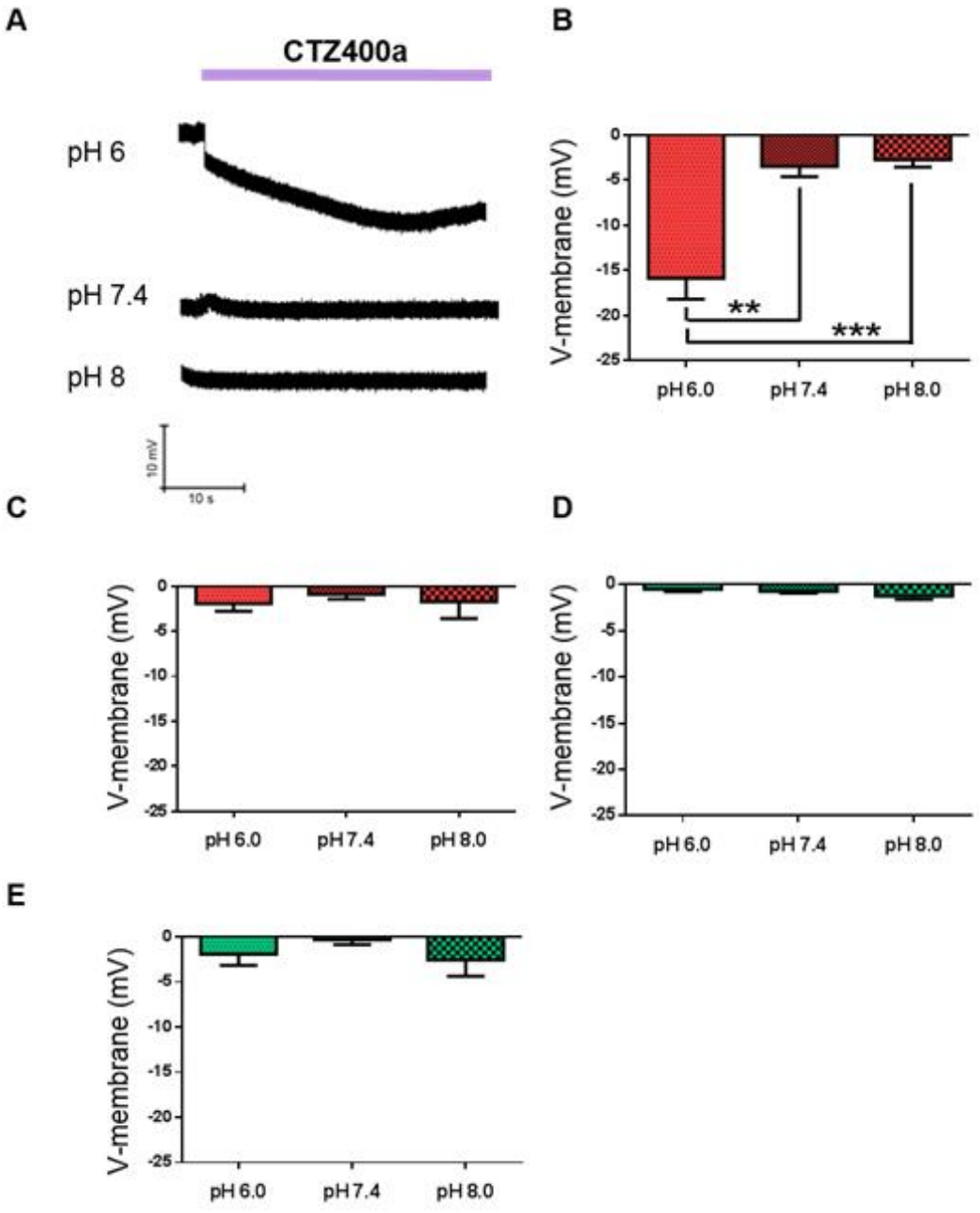

Figure 10. Determination of pHIL activity in HEK293T cells. (A-B) Representative plots of current clamp recordings (mV/s) from HEK293T cells expressing pHIL show plasma membrane hyperpolarization in response to CTZ 400a (10 µM) and upon intracellular acidification (A). The graph in (B) shows the absence of hyperpolarization in HEK293T expressing the ctrl probe. Mean ± SEM of n=12, 9, 8 cells for pH 6, 7.4 and 8, respectively; ** $p<0.01$, *** $p<0.001$, one-way ANOVA followed by Bonferroni's post-hoc test. (C-D) Representative plots of current clamp recordings from HEK293T cells expressing pHIL (C) or the ctrl probe (D) show no plasma membrane hyperpolarization in response to coelenterazine h (20 µM) and after intracellular acidification. Mean ± SEM of n=6 cells. $p>0.05$, one-way ANOVA.

4.5 Validation of pHIL and ctrl -expressing AAVs expression and localization in primary hippocampal neurons.

After the cloning of pAAV2-pHIL and pAAV2- ctrl, AAV2/9 particles were produced (TIGEM, AAV Vector Core) and primary hippocampal neurons infected. First, a western blot analysis was performed by using antibodies against E^2GFP. As shown in [**Figure 11B**], the fusion proteins have a molecular weight of 93 kDa and 62 kDa respectively, as expected. In order to verify the localization of the two probes, neurons expressing pHIL or the ctrl probe were fixed and stained with antibodies against E^2GFP. Confocal microscopy analysis revealed the localization of pHIL in correspondence of the plasma membrane [**Figure 11C** *lower panel*], while the ctrl probe was observed in the cytoplasm [**Figure 11C** *upper panel*].

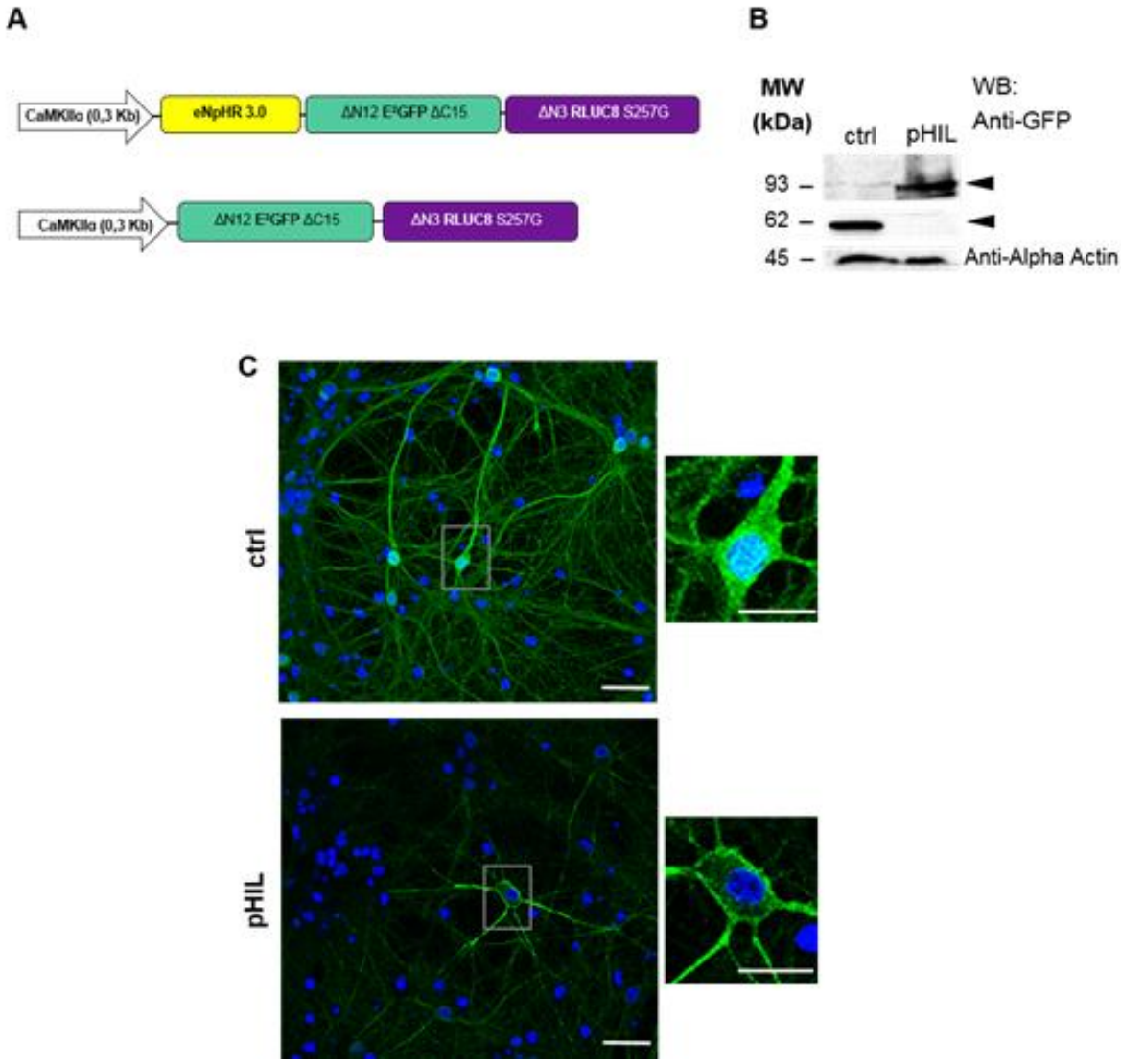

Figure 11. **pHIL and pHIL control structure, expression and localization in hippocampal neurons.** (A) Schematic illustration of pHIL and control AAV constructs. For details see text. Both fusion proteins are expressed under the control of the truncated form (0.3 Kb) of the CaMKIIα promoter. (B) Western blot analysis of hippocampal neurons expressing pHIL and control. The expression of the fusion proteins (arrowheads) was analyzed using anti-GFP antibodies. Anti-alpha actin antibodies were used to verify equal loading. (C) Representative confocal images showing the membrane localization of pHIL (lower panel) and the cytoplasmic localization of the control probe (upper panel). E^2GFP fluorescence, green channel; Hoechst-labeled nuclei, blue channel. Scale bars: 25 µm for pHIL and 20 µm for the control in lower magnification images; 5 µm in higher magnification images.

4.6 Analysis of pH_i changes during epileptic like conditions.

pHIL is activated only under acidic conditions. It is known that, during seizure activity, neurons accumulate H^+, resulting in acidification of the intracellular space (Xiong et al., 2000). To test the activation of pHIL also in hippocampal neurons, we used bicuculline, a competitive antagonist of $GABA_A$ receptors. Recent studies described the bicuculline-induced extracellular acidification at cell bodies and at synapses (Chiacchiaretta et al., 2017). Following a similar approach, we tested whether bicuculline was able to induce also an intracellular acidification. To do this, we engineered the pH sensor E^2GFP to monitor intracellular pH shifts (pH_i). ΔN12-E^2GFP-ΔC15 was inserted downstream of the human cluster of differentiation 4 (CD4) receptor transmembrane sequence, to target the E^2GFP to the intracellular side of the plasma membrane, under the control of the human ubiquitin promoter (hUb), in a lentiviral vector (pLenti) **[Figure 12A**].

The reason for which we cannot use pHIL to monitor intracellular pH shifts in plasma membrane is that the eNpHR3.0 will absorb the great part of the light emitted by the ΔN12-E^2GFP-ΔC15, hiding the possible bicuculline effect.

First, a western blot analysis was performed in order to analyze the expression of CD4--ΔN12-E^2GFP-ΔC15 and control (E^2GFP only from pcDNA-E^2GFP, provided by Dr. Bizzarri, University of Pisa) in HEK293T cells by using antibodies against E^2GFP. As shown in [**Figure 12B**], the fusion protein has a molecular weight of 78 kDa, as expected. In order to verify the localization of the probe, confocal cell imaging was performed in HEK293T cells and primary hippocampal neurons transfected with the pLenti-CD4-ΔN12-E^2GFP-ΔC15 and control plasmids. Cells were fixed and stained with antibodies against E^2GFP. Confocal microscopy analysis revealed the localization of CD4-ΔN12-E^2GFP-ΔC15 in correspondence of the plasma membrane both in in HEK293T cells and in primary hippocampal neurons

[**Figure 12C and D**, *upper panel*], while the ctrl probe was observed in the cytoplasm [**Figure 12C and D**, *lower panel*].

Time-lapse confocal live cell imaging was subsequently used to study bicuculline-induced intracellular acidification in hippocampal neurons. Hippocampal primary neurons were plated on 25 mm poly-L-lysine coated glass coverslips and after 7 DIV were transfected with pLenti-CD4-ΔN12-E^{2}GFP-ΔC15. The bicuculline treatment was performed at DIV 10, changes in fluorescence were monitored and pH values were subsequently extrapolated from ratio values using a calibration curve created before every experiment. A scheme of the time course of the experiments is shown in [**Figure 12E**]: pH was first measured under baseline conditions (2 min), then network hyperactivity was induced by blocking $GABA_A$ receptors with bicuculline (30 μM) and cultures were imaged for further 8 min. An increase in E^{2}GFP fluorescence (λ_{ex} = 405 nm) was observed during the bicuculline treatment, in correspondence of discrete spots along neurite extensions [**Figure 12F**]. To quantify the variation in fluorescence intensity, regions of interest (ROIs) of about 2 μm were drawn around the spots in the neurite extensions, and mean fluorescence intensity values were calculated for every image at every time point for the 405 nm and 488 nm excitation. Emission fluorescence ratios were converted to pH values according to the calibration curves collected by fitting each ratio value in a sigmoidal dose response curve using the Graphpad Prism 7.04 software. [**Figure 12G**] shows pHi variations upon the addition of bicuculline. Under basal conditions pHi was 7.3, while in the presence of bicuculline pHi values constantly dropped to reach a plateau value of 6.1 after about 7 min.

To demonstrate that the decrease in pH is due to the bicuculline action and not to the bleaching effect, live cell imaging of hippocampal neurons transfected with pLenti-CD4-ΔN12-E^{2}GFP-ΔC15 was performed for 10 minutes without the addition

of bicuculline. [**Figure 12H**] show no decrease in pH during all the experiment demonstrating that the decrease in pH observed before is due to the action of bicuculline.

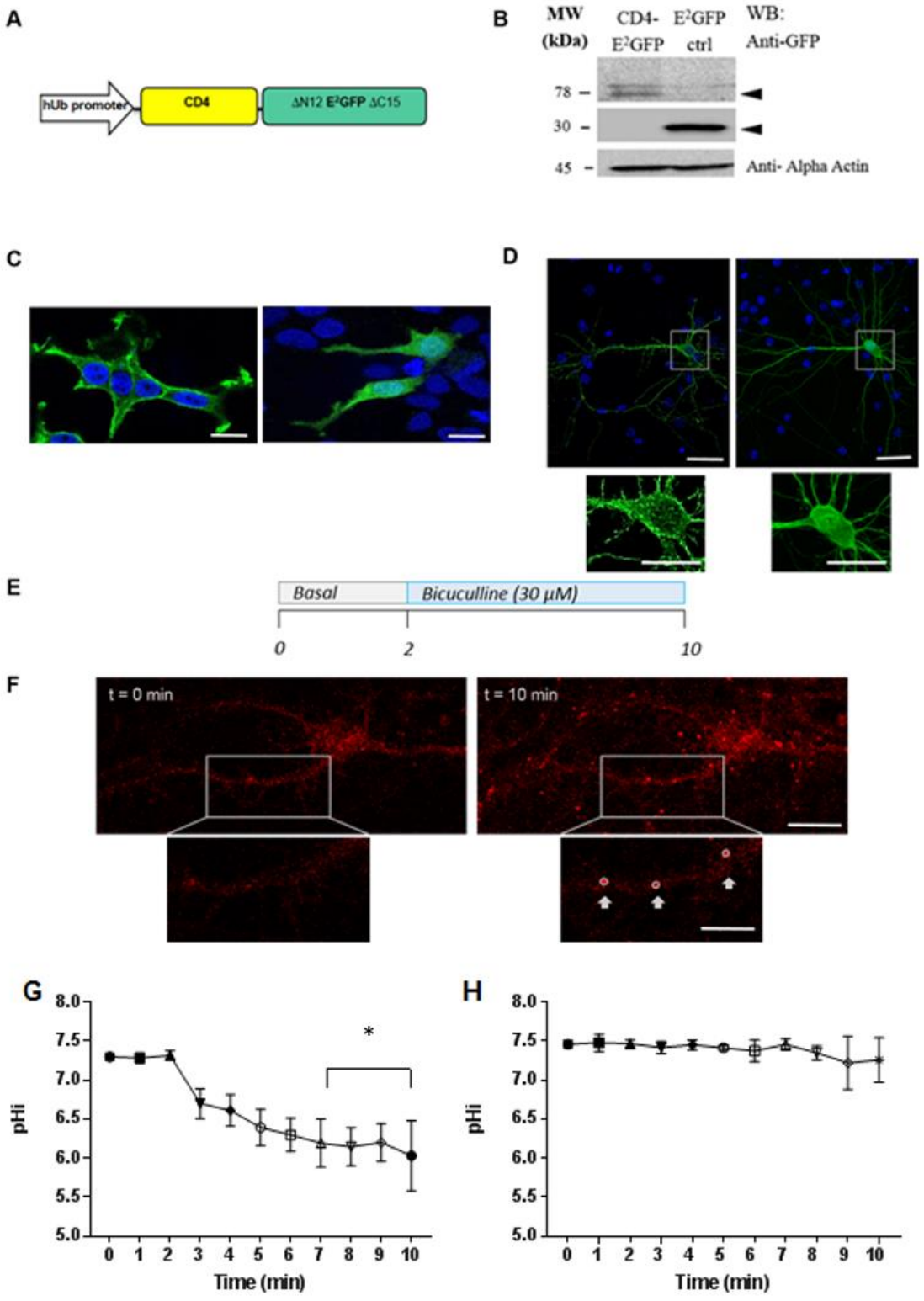

Figure 12. **pH_i variations under epileptic-like conditions**. (A) Schematic illustration of the Ub-CD4/E^2GFP probe. For details, see text. The fusion protein expression is under the control of the human ubiquitin promoter. (B) Western blot analysis of HEK293T cells expressing CD4/E^2GFP and control (E^2GFP only) probes. The expression of the fusion

proteins was analyzed using anti-GFP antibodies. Anti-alpha actin antibodies were used to verify equal loading. (C-D) Representative confocal images of the membrane localization of CD4/E^{2}GFP in HEK293T cells and in hippocampal neurons (C, D, left). As a control, the cytoplasmatic E^{2}GFP was used (C, D right). E^{2}GFP fluorescence, green channel; Hoechst-labeled nuclei, blue channel. Scale bars: 20 µm in lower magnification images; 5 µm in higher magnification images. (E) Schematic representation of the time course of a typical experiment with the addition of bicuculline (30 µM) after 2 min of imaging under basal conditions. (F) Representative fluorescence (λex = 405 nm) images taken from neurons under basal conditions (t = 0 min) and after bicuculline treatment (t = 10 min). ROIs used for quantification are indicated in the high-magnification images (indicated by arrows). Scale bars, 20 µm for low magnification images and 5 µm for high magnification images. (G) The graph illustrates pH variations upon bicuculline (30 µM) addition. pHi decreases as a function of time in discrete spots along cell extensions. Mean ± SEM, n=7 independent preparations, * $p < 0.05$ compared to basal levels (0-2 min) One way ANOVA for repeated measures, followed by Friedman's post-hoc test. (H) The graph illustrates possible pH variations due to the bleaching effect during the entire time of the experiments. Mean ± SEM, n=3 cells.

4.7 Electrophysiological characterization of pHIL in primary hippocampal neurons.

Bicuculline is able to induce intracellular acidification and to mimic the epileptic phenotype increasing hippocampal neurons excitability. In order to analyze the functioning of pHIL in primary neurons, primary hippocampal neurons were infected with the AAV2/9 pHIL and cell-attached voltage-clamp recordings was performed after treatment with tyrode alone [**Figure 13A**], tyrode with bicuculline (30 µM) [**Figure 13B**] and tyrode with bicuculline (30 µM) and CTZ400a (40 µM) [**Figure 13C**]. The cell attached electrophysiological technique was used instead of patch clamp, as the latter involves the buffering of neuronal cytoplasm, which would abolish bicuculline-induced intracellular acidification, thus impairing the activation of the probe.

Preliminary data suggest that pHIL activation is able to reduce bicuculline-induced excitability in primary neurons, in particular the number of bursts [**Figure 13D**], the intra-burst frequency [**Figure 13E**] and the number of intra-burst events [**Figure 13F**] are decreased after the treatment with bicuculline and CTZ400a with respect to cells treated with bicuculline alone.

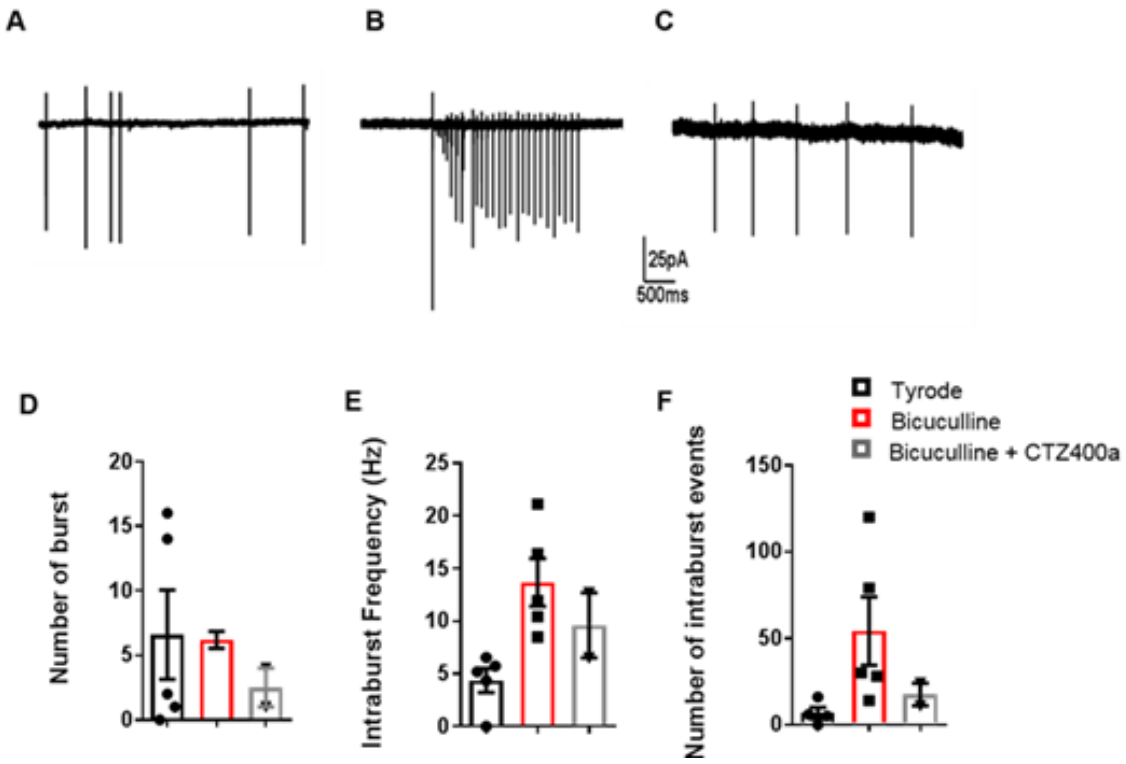

Figure 13. **pHIL activation inhibits bicuculline-induced hyperexcitability in hippocampal neurons**. Representative traces of cell-attached voltage-clamp recordings of primary hippocampal neurons infected with AAV2/9-pHIL in the presence of tyrode (A), bicuculline 30 µM (B), and bicuculline 30 µM + CTZ400a 40µM (C). Graphs show number of burst (D), intraburst frequency (E) and number of intraburst events (F) under the three experimental conditions. Mean ± SEM, n=5 neurons from one preparation.

5. Discussion

Seizures are temporary changes of neuronal activity in the brain characterized by high neuronal excitability, and when repeated chronically, they are a typical symptom of epilepsy. A number of drugs are currently available to reduce the hyperexcited state in epileptic patients, but unfortunately, in many cases medications are unable to adequately control seizures. For many "drug resistant" patients the surgery can significantly reduce or eliminate seizures but for the other part of them seizures continue to impair their daily life.

An alternative option to control seizures can be the brain stimulation of various brain areas. Open loop neural stimulation such as VNS (vagus nerve stimulation), TNS (trigeminal nerve stimulation) or DBS (deep brain stimulation) consist in the application of electric currents to seizure-generating circuitries in a continuous mode and have been shown to reduce seizure frequency after two years[63]. Although such open loop neuromodulation is in some cases efficient to treat seizures, it involves the long-term continuous stimulation and it can affect many parts of the brain increasing the possible risk of side effects.

A possible alternative is the closed loop neuromodulation. In this case the system delivers stimulation through electrodes placed in brain areas shown to generate seizures. The stimulation starts when it detects, through the EEG, the beginning of seizure activity. It is known that closed loop transcranial cortical stimulation in rats consistently interrupt seizures for six weeks, reduce the seizure duration and more importantly no adverse effects are observed on the electrophysiologic activity of the brain after the treatment[64]. However, despite many positive effects of the closed loop neurostimulation, significantly higher seizure rate

is still observed during the treatment and a high rate of complications are reported within the first month of implantation[65].

Despite important advancements, refractory epilepsies still represent a serious problem. For this reason, novel possible approaches for epilepsy treatment are being investigated, amongst which gene therapy. Gene therapy in the nervous system involves the transfer and the expression of particular genes in brain cells using mainly adeno associated viral vectors (AAV). Genes transferred in neurons after viral infection may code for proteins able to modulate neuronal activity. This is the case of *opsins* and *optogenetics*. Optogenetics provide immediate transient control of specific cell populations using light sensitive proteins, named opsins[38].In vitro and in vivo studies indicate that optogenetics can be used to control seizure activity[46]. Moreover, recently, closed loop neuromodulation has been combined to optogenetics. In this case, in mice expressing two different opsins (ChR and HR), seizures can be detected in real time and stopped. The detection of seizures in real time is due to implantation of intrahippocampal depth electrodes and optogenetic mediated seizures control is due to the activation of opsin mediated by individual optical fibers[47] .

The very important concept at the basis of the optogenetic approach is the precise spatiotemporal wavelength-specific illumination that is achieved, usually, using optical fibers or using LED light sources. However, the implementation of such techniques requires specialized equipment, the surgical implantation is very invasive and, above all, the optogenetic approach is restricted to small volumes of the brain because of the difficulty to illuminate deep brain areas. In this scenario, *luminopsins* get ahead[53]. Luminopsin can modulate neural activity in a closed loop fashion and thus be activated only when it is needed through direct opsin stimulation or upon addition of luciferase substrate. This last aspect is important because it could provide an alternative to the use of external light sources used to activate opsins. It is known

that luminopsins can be used to suppress in an efficient way epileptic seizures in both vitro and in vivo[51]. In this last case is demonstrated that after the addition of the chemical compound able to activate luminopsin (coelenterazine), neuronal activity is suppressed in excitatory neurons expressing the luminopsin[51]. In this thesis, we want to implement a similar strategy to try to control epileptic seizures.

We aimed to engineer a probe in which a bioluminescent protein was coupled with an inhibitory opsin, the *Natromonas Pharaonis* Halorhodopsin, with the purpose of reducing the hyperexcitability of excitatory neurons under epileptic conditions. The expression of the probe is confined to excitatory neurons thanks to the use of the specific CaMKIIα promoter. Moreover, this model is constructed on the model of the *closed loop neurostimulation* because the inhibition of excitatory neurons expressing the probe occurs when and where needed, upon neurons intracellular acidification, phenomenon observed during epileptic conditions[15,16], thanks to the pH-sensitive variant of GFP, E^2GFP[22] . Thus, the chimeric protein called *pH sensitive inhibitory luminopsin (pHIL)* was engineered. It takes advantage of the BRET mechanism between the RLuc8 and the E^2GFP to increase the power density of emitted light[52] directed to the eNpHR3.0 and to give to the probe pH sensitivity. The pH sensitivity is linked not only to the acidic environment but also to the wavelength of the light emitted by the luciferase. For this reason, the search of a specific variant of the luciferase substrate is the key point at the base of the functioning of the probe. E^2GFP is able to emit green light (λ_{em}=510 nm) in an acidic environment upon illumination with 405 nm light. RLuc8 is able to emit near-UV light upon reaction with the coelenterazine variant CTZ400a[57].

Neurons transduced with pHIL are in principle unaffected in the absence of the specific substrate and only affected when the substrate is present, thereby avoiding permanent alteration of their properties and then, interestingly, the near-UV emission

is a transient effect (in the order of few minutes) linked to the reaction of CTZ400a with the RLuc8 enzyme. This is a great advantage because, in this way, it should not be deleterious to neurons and to the brain. Using this substrate, pHIL is able to hyperpolarize HEK293T cells specifically under acidic conditions upon addition of CTZ400a, despite it is known that E^2GFP is able to emit a bit also in a neutral pH[22].In this case, however, the fluorescence emitted by E^2GFP is not enough to activate eNpHR3.0 (Fig.10B). It is remarkable that the quantity of light emitted, the hyperpolarization rate and the time of pHIL activation depend on the probe expression at plasma membrane but also on the CTZ400a concentration used. This is interesting because, when pHIL is expressed in excitatory neurons, we can obtain the modulation of neuronal activity by limiting CTZ400a concentration. This should avoid the risk of changing $GABA_A$ receptor reversal potential, mediated by eNpHR3.0 after photostimulation, which may result in increased excitability[66].

pHIL can therefore be considered a promising chemo-genetics approach to achieve cell-specific on demand seizure suppression. Such approach is reminiscent of the DREADD (Designer Receptors Exclusively Activated by Designer Drugs) technology that has been used to treat and attenuate focal neocortical seizures[67].The DREADD approach is based on the cell-specific expression of a receptor that is activated by a drug, the clozapine-N-oxide (CNO). Despite the use of DREADDs is promising, their use has some disadvantages. For example, DREADDs need the activation of secondary endogenous signaling proteins (G proteins), which should be present in every target population of neurons; the effects of DREADD activation can have very diverse and undesired effects other than altering membrane conductance; clozapine (CNO) metabolism has multiple effects on the brain and for this reason clinical translation is prohibitive[51] .

This is not the case of pHIL. Everything required to manipulate neural activity is encoded in a single molecule; CTZ h and CTZ400a are used for in vivo imaging and no side effects have been reported[52,68] ;no downstream side-effects re reported after the activation of luminopsins[51]. Despite many advantages, some aspects may make the translational clinical application of pHIL to treat epilepsy difficult, the most important being the use of the gene therapy. Gene therapy would involve the use of viral vectors, in our case, adeno associated viral vectors, which can be immunogenic. Furthermore, the expression of opsins, in our case of eNpHR3.0, can be difficult because the opsin derive from Natronomonas Pharaonis, an archaea evolutionarily far from humans.

In conclusion, in this thesis we propose a very interesting and exciting chemo-optogenetic approach to detecting and potentially treating epileptic seizures. This approach could sign the way of closed loop therapies for the treatment of drug resistant epilepsies.

In the first part of the work, we engineered pHIL and characterized it, with success, in cell lines (HEK293T). The following step was to characterize it also in primary hippocampal neurons. To do this we characterized bicuculline-induced intracellular acidification, which localized to discrete boutons, where pH_i decreased as a function of time. Using the bicuculline model, it is therefore possible to analyze the capability of *pHIL* to modulate the hyperexcitated state in primary neurons in vitro.

In this case, the cell-attached electrophysiological technique was used to avoid the buffering of neurons intracellular side using the classic patch clamp technique, which would abolish the bicuculline induced intracellular acidification necessary to activate the probe. Preliminary data suggest that in primary hippocampal neurons infected with AAV2/9-pHIL, the addi tion of CTZ400a is able to reduce the

bicuculline-induced increase the number of bursts, the intraburst frequency and the number of intraburst events with respect to basal conditions (tyrode). Remarkably, pHIL activation reduced the previously described parameters to a value similar or lower with respect to the basal condition. The analysis of pHIL capability to modulate bicuculline-induced hippocampal neurons hyperactivation is a work in progress. Another ongoing experiment is that to analyze the effect of pHIL by looking at the network activity of neurons infected with the AAV2/9- pHIL using Multi Electrode Arrays (MEA).

For the in vivo characterization of *pHIL*, first the expression and the localization of the probe in the hippocampal cells will be studied. This goal will be achieved through the stereotaxic injection of AAV2/9 particles carrying *pHIL* in the dorsal hippocampus. Then, in order to know how much time CTZ400a needs to reach the dorsal hippocampus and activate pHIL, live bioluminescence imaging on AAV2/9-pHIL injected mice will be performed. This goal is indispensable because we need to determine the time window in which we can inject the kainic acid and to induce seizures, mimicking the temporal lobe epilepsy. Temporal lobe epilepsy will be reproduced after injection of kainic acid in the hippocampus of mice expressing pHIL. The pHIL mediated control of epileptic activity induced by kainic acid will be possible upon injection of CTZ400a, which is able to cross the blood brain barrier[68]. We will demonstrate to what extent pHIL is able to control seizures by employing behavioural tests and EEG recordings in pHIL- and Ctrl injected mice. The in vivo experiments will provide support to the hypothesis that chemogenetics can be effectively used to modulate seizure propagation, thus laying the basis for the development of novel therapeutic approaches.

6. Bibliography

1. Denker, S. P. & Barber, D. L. Cell migration requires both ion translocation and cytoskeletal anchoring by the Na-H exchanger NHE1. *J. Cell Biol.* 159, 1087–1096 (2002).

2. Putney, L. K. & Barber, D. L. Na-H Exchange-dependent Increase in Intracellular pH Times G2/M Entry and Transition. *J. Biol. Chem.* 278, 44645–44649 (2003).

3. Cano Abad, M. F., Di Benedetto, G., Magalhães, P. J., Filippin, L. & Pozzan, T. Mitochondrial pH Monitored by a New Engineered Green Fluorescent Protein Mutant. *J. Biol. Chem.* 279, 11521–11529 (2004).

4. Tombaugh, G. C. & Somjen, G. G. Differential sensitivity to intracellular pH among high- and low- threshold Ca2+ currents in isolated rat CA1 neurons. *J. Neurophysiol.* 77, 639–653 (1997).

5. Tsukioka, M., Iino, M. & Endo, M. pH dependence of inositol 1,4,5-trisphosphate-induced Ca2+ release in permeabilized smooth muscle cells of the guinea-pig. *J. Physiol.* 475, 369–375 (1994).

6. Jianjie Ma , Michael Fill , C . Michael Knudson , Kevin P . Campbell and Roberto Coronado. Ryanodine Receptor of Skeletal Muscle Is a Gap Junction--Type Channel. American Association for the Advancement of Science Stable URL : h. 242, 99–102 (2016).

7. Tang, C. M., Dichter, M. & Morad, M. Modulation of the N-methyl-D-aspartate channel by extracellular H+. *Proc. Natl. Acad. Sci. U. S. A.* 87, 6445–6449 (1990).

8. Lei, S., Orser, B. A., Thatcher, G. R. L., Reynolds, J. N. & Macdonald, J. F. Positive allosteric modulators of AMPA receptors reduce proton-induced receptor desensitization in rat hippocampal neurons. *J. Neurophysiol.* 85, 2030–2038 (2001).

9. Pasternack, M., Voipio, J. & Kaila, K. Intracellular carbonic anhydrase activity and its role in GABA-induced acidosis in isolated rat hippocampal pyramidal neurones. *Acta Physiol. Scand.* 148, 229–231 (1993).

10. Casey, J. R., Grinstein, S. & Orlowski, J. Sensors and regulators of intracellular pH. *Nat. Rev. Mol. Cell Biol.* 11, 50–61 (2010).

11. Raley-Susman, K. M., Cragoe Jr., E. J., Sapolsky, R. M. & Kopito, R. R. Regulation of intracellular pH in cultured hippocampal neurons by an amiloride-insensitive Na+/H+ exchanger. *J Biol Chem* 266, 2739–2745 (1991).

12. Park, H. J., Rajbhandari I., Yang H. S., Lee S., Cucoranu D., Cooper D. S., Choi I.. Neuronal expression of sodium/bicarbonate cotransporter NBCn1 (SLC4A7) and its response to chronic metabolic acidosis. *Am. J. Physiol. - Cell Physiol.* 298, 1018–1028 (2010).

13. Verma, V., Bali, A., Singh, N. & Jaggi, A. S. Implications of sodium hydrogen exchangers in various brain diseases. *J. Basic Clin. Physiol. Pharmacol.* 26, 417–426 (2015).

14. Gu, X. Q., Yao, H. & Haddad, G. G. Increased neuronal excitability and seizures in the Na+/H+ exchanger null mutant mouse. *Am. J. Physiol. - Cell Physiol.* 281, 496–503 (2001).

15. Ahmed, Z. & Connor, J. A. Intracellular pH changes induced by calcium influx during electrical activity in molluscan neurons. *J Gen Physiol* 75, 403–426 (1980).

16. Xiong, Z.-Q. Z., Saggau, P. & Stringer, J. L. J. Activity-Dependent Intracellular Acidification Correlates with the Duration of Seizure Activity. *J. Neurosci.* 20, 1290–1296 (2000).

17. Caldwell, P. An investigation of the intracellular pH of crab muscle fibres by means of micro-glass and micro-tungsten electrodes. *J Physiol* 126, 169–180 (1954).

18. Miesenböck, G., De Angelis, D. A. & Rothman, J. E. Visualizing secretion and synaptic transmission with pH-sensitive green fluorescent proteins. *Nature* 394, 192–195 (1998).

19. Sankaranarayanan, S., De Angelis, D., Rothman, J. E. & Ryan, T. A. The Use of pHluorins for Optical Measurements of Presynaptic Activity. *Biophys. J.* 79, 2199–2208 (2000).

20. Mahon, M. J. pHluorin2: an enhanced, ratiometric, pH-sensitive green florescent protein. Adv Biosci Biotechnol. NIH Public Access. 2, 132–137 (2011).

21. Hanson, G. T., McAnaney T. B., Park E. S., Rendell M. E. P., Yarbrough D. K., Chu S., Remington, S. J. Green fluorescent protein variants as ratiometric dual emission ph sensors. 1. Structural characterization and preliminary application. *Biochemistry* 41, 15477–15488 (2002).

22. Bizzarri, R., Arcangeli C., Arosio D., Ricci F., Faraci P., Cardarelli F., & Beltram F. Development of a novel GFP-based ratiometric excitation and emission pH indicator for intracellular studies. *Biophys. J.* 90, 3300–14 (2006).

23. Chiacchiaretta, M., Latifi S., Bramini M. , Fadda M. ,Fassio A., Benfenati F.,Cesca F. Neuronal hyperactivity causes Na+/H+ exchanger-induced extracellular acidification at active synapses. *J. Cell Sci.* 130, 1435–1449 (2017).

24. Raimondo, J. V., Irkle, A., Wefelmeyer, W., Newey, S. E. & Akerman, C. J. Genetically encoded proton sensors reveal activity-dependent pH changes in neurons. *Front. Mol. Neurosci.* 5, 1–12 (2012).

25. Staley, K. J., Soldo, B. L. & Proctor, W. R. Ionic mechanisms of neuronal excitation by inhibitory GABAA receptors. *Science (80-.).* 269, 977–981 (1995).

26. Trevelyan, A. J. & Schevon, C. A. How inhibition influences seizure propagation. *Neuropharmacology* 69, 45–54 (2013).

27. Löshcer, W. Animal models of epilepsy for the development of antiepileptogenic and disease-modifying drugs. A comparison of the pharmacology of kindling and post-status epilepticus models of temporal lobe

epilepsy. *Epilepsy Res.* 50, 105–123 (2002).

28. Paz, J. T., Bryant A.S., Peng K., Fenno L., Yizhar O., Frankel W.N., Deisseroth K., Huguenard J.R.. A new mode of corticothalamic transmission revealed in the Gria4 -/- model of absence epilepsy. *Nat. Neurosci.* 14, 1167–1175 (2011).

29. Lévesque, M., Avoli, M. & Bernard, C. Animal models of temporal lobe epilepsy following systemic chemoconvulsant administration. *J. Neurosci. Methods* 260, 45–52 (2016).

30. Carriero, G., Arcieri S., Cattalini, A., Corsi L., Gnatkovsky V., & De Curtis M. A guinea pig model of mesial temporal lobe epilepsy following nonconvulsive status epilepticus induced by unilateral intrahippocampal injection of kainic acid. *Epilepsia* 53, 1917–1927 (2012).

31. Curtis, D. R., Felix, D. & McLellan, H. GABA and hippocampal inhibition. *Br. J. Pharmacol.* 40, 881–883 (1970).

32. Baram, T. Z. & Snead, O. C. Bicuculline induced seizures in infant rats: ontogeny of behavioral and electrocortical phenomena. *Dev. Brain Res.* 57, 291–295 (1990).

33. Amna Rana and Alberto E. Musto. The role of inflammation in the development of epilepsy. *Transplant. Proc.* 29, 2583–2584 (1997).

34. Fisone, G., Langel U., Carlquist M., Bergman T., Consolo S., Hökfelt T., Bartfai T. Galanin receptor and its ligands in the rat hippocampus. *Eur. J. Biochem.* 181, 269–276 (1989).

35. Mazarati, A. M., Liu H., Soomets U., Sankar R., Shin D., Katsumori H., Wasterlain C.G. Galanin modulation of seizures and seizure modulation of hippocampal galanin in animal models of status epilepticus. *J. Neurosci.* 18, 10070–10077 (1998).

36. Sørensen, A. T. & Kokaia, M. Novel approaches to epilepsy treatment. *Epilepsia* 54, 1–10 (2013).

37. Zemelman, B. V., Lee, G. A., Ng, M. & Miesenböck, G. Selective photostimulation of genetically chARGed neurons. *Neuron* 33, 15–22 (2002).

38. Boyden, E. S., Zhang, F., Bamberg, E., Nagel, G. & Deisseroth, K. Millisecond-timescale, genetically targeted optical control of neural activity. *Nat. Neurosci.* 8, 1263–1268 (2005).

39. Zhang F., Wang L.P., Brauner M., Liewald J. F., Kay K., Watzke N., Deisseroth K. Multimodal fast optical interrogation of neural circuitry. *Nature* 446, 633–639 (2007).

40. Nagel, G., Szellas T., Huhn W., Kateriya S., Adeishvili N., Berthold P., Bamberg E. Channelrhodopsin-2, a directly light-gated cation-selective membrane channel. *Proc. Natl. Acad. Sci. U. S. A.* 100, 13940–13945 (2003).

41. Gradinaru, V., Mogri, M., Thompson, K. R., Henderson, J. M. & Deisseroth, K. Optical Deconstruction of Parkinsonian Neural Circuitry. 324, 354–359 (2009).

42. Funken, M., Malan, D., Sasse, P. & Bruegmann, T. Optogenetic hyperpolarization of cardiomyocytes terminates ventricular arrhythmia. *Front. Physiol.* 10, 1–7 (2019).

43. Shengli Zhao, Jonathan T. Ting1, Hisham E. Atallah, Li Qiu, Jie Tan, B., Gloss, George J. Augustine, Karl Deisseroth, Minmin Luo, Ann M. Graybiel, A. & Feng, G. HHS Public Access. *Physiol. Behav.* 176, 139–148 (2017).

44. Trombin, F., Gnatkovsky, V. & de Curtis, M. Changes in action potential features during focal seizure discharges in the entorhinal cortex of the in vitro isolated guinea pig brain. *J. Neurophysiol.* 106, 1411–1423 (2011).

45. Gradinaru, V., Zhang F., Ramakrishnan C., Mattis J., Prakash R., Diester I., Deisseroth K. *et al.* Molecular and Cellular Approaches for Diversifying and Extending Optogenetics. *Cell* 141, 154–165 (2010).

46. Tønnesen, J., Sørensen, A. T., Deisseroth, K., Lundberg, C. & Kokaia, M. Optogenetic control of epileptiform activity. *Proc. Natl. Acad. Sci. U. S. A.* 106, 12162–7 (2009).

47. Krook-Magnuson, E., Armstrong, C., Oijala, M. & Soltesz, I. On-demand optogenetic control of spontaneous seizures in temporal lobe epilepsy. *Nat. Commun.* 4, 1–8 (2013).

48. Tønnesen, J. & Kokaia, M. Epilepsy and optogenetics: Can seizures be controlled by light? *Clin. Sci.* 131, 1605–1616 (2017).

49. Zhang, J., Laiwalla F., Kim J. A., Urabe H., Wagenen R. Van, Song Y., Arto V. Integrated device for optical stimulation and spatiotemporal electrical recording of neural activity in light-sensitized brain tissue. *J Neural Eng* 6, (2009).

50. Wang, J., Wagner F., Borton D. A., Zhang J., Ozden I., Burwell R. D., Deisseroth K. Integrated device for combined optical neuromodulation and electrical recording for chronic in vivo applications. *J. Neural Eng.* 9, (2012).

51. Tung, J. K., Gutekunst, C.-A. & Gross, R. E. Inhibitory luminopsins: genetically-encoded bioluminescent opsins for versatile, scalable and hardware-independent optogenetic inhibition. *Sci. Rep.* 5, 14366 (2015).

52. Saito, K., Chang Y.F., Horikawa K., Hatsugai N., Higuchi Y., Hashida M., Nagai T. Luminescent proteins for high-speed single-cell and whole-body imaging. *Nat. Commun.* 3, 1262 (2012).

53. Berglund K., Birkner E., Augustine G.J., Hochgeschwender U. 2013. Light-Emitting Channelrhodopsins for Combined Optogenetic and Chemical-Genetic Control of Neurons. *FEBS Lett.* 587, 1923–1928 (2013).

54. Nakatsu, T., Ichiyama S., Hiratake J., Saldanha A., Kobashi N., Sakata K. & Kato H. Structural basis for the spectral difference in luciferase bioluminescence. *Nature* 440, 372–376 (2006).

55. Land, B. B., Brayton, C. E., Furman, K. E., LaPalombara, Z. & Di Leone, R. J. Optogenetic inhibition of neurons by internal light production. *Front. Behav. Neurosci.* 8, 1–6 (2014).

56. Loening, A. M., Wu, A. M. & Gambhir, S. S. Red-shifted Renilla reniformis

luciferase variants for imaging in living subjects. *Nat. Methods* 4, 641–643 (2007).

57. Shimomura, O., Kishi, Y. & Inouye, S. The relative rate of aequorin regeneration from apoaequorin and coelenterazine analogues. *Biochem. J.* 296, 549–551 (1993).

58. Hart, R. C., Matthews, J. C., Hori, K. & Cormier, M. J. Renilla reniformis Bioluminescence: Luciferase-Catalyzed Production of Nonradiating Excited States from Luciferin Analogues and Elucidation of the Excited State Species Involved in Energy Transfer to Renilla Green Fluorescent Protein. *Biochemistry* 18, 2204–2210 (1979).

59. Tung, J. K., Shiu, F. H., Ding, K. & Gross, R. E. Chemically activated luminopsins allow optogenetic inhibition of distributed nodes in an epileptic network for non-invasive and multi-site suppression of seizure activity. *Neurobiol. Dis.* 109, 1–10 (2018).

60. Borroto-Escuela, D. O., Flajolet, M., Agnati, L. F., Greengard, P. & Fuxe, K. Bioluminescence Resonance Energy Transfer Methods to Study G Protein-Coupled Receptor-Receptor Tyrosine Kinase Heteroreceptor Complexes. *Methods in Cell Biology* 117, (Elsevier Inc., 2013).

61. Dong, J., Fan, P., Frizzell, R. A. & Al, D. E. T. Quantitative Analysis of the Packaging Capacity Recombinant Adeno-Associated Virus of. 2112, 2101–2112 (1996).

62. Hioki, H., Kameda H., Nakamura H., Okunomiya T., Ohira K., Nakamura K., Kuroda M. , Furuta T. and Kaneko T. Efficient gene transduction of neurons by lentivirus with enhanced neuron-specific promoters. *Gene Ther.* 14, 872–882 (2007).

63. Sisterson, N. D., Wozny, T. A., Kokkinos, V., Constantino, A. & Richardson, R. M. Closed-Loop Brain Stimulation for Drug-Resistant Epilepsy: Towards an Evidence-Based Approach to Personalized Medicine. *Neurotherapeutics* 16, 119–127 (2019).

64. Kozák, G. & Berényi, A. Sustained efficacy of closed loop electrical stimulation for long-term treatment of absence epilepsy in rats. *Sci. Rep.* 7, 1–10 (2017).

65. Morrell, M. J. Responsive cortical stimulation for the treatment of medically intractable partial epilepsy. *Neurology* 77, 1295–1304 (2011).

66. Raimondo, J. V., Kay, L., Ellender, T. J. & Akerman, C. J. Optogenetic silencing strategies differ in their effects on inhibitory synaptic transmission. *Nat. Neurosci.* 15, 1102–1104 (2012).

67. Kätzel, D., Nicholson, E., Schorge, S., Walker, M. C. & Kullmann, D. M. Chemical-genetic attenuation of focal neocortical seizures. *Nat. Commun.* 5, (2014).

68. Nishihara, R., Paulmurugan R., Nakajima T., Yamamoto E., Natarajan A., Afjei R., Hiruta Y., Iwasawa N., Nishiyama S., Citterio D., Sato M., Kim SB., Suzuki K. Highly bright and stable NIR-BRET with blue-shifted

coelenterazine derivatives for deep-tissue imaging of molecular events in vivo. *Theranostics* 9, 2646–2661 (2019).

Acknowledgments

The PhD is not only something that allow you to grow in the professional point of view but it is a school of life.

The very important thing that I learned is the *resilience*. In everyday research life, you try and you fail. I learned to grow thanks to my mistakes and to do not give up.

I would like to thank first the Prof. Fabio Benfenati for giving me the opportunity to do my PhD thesis in his laboratory and for the trust he had in me despite all the difficulties I met in carrying out my thesis project.

I want to explain all my gratitude to Dr. Fabrizia Cesca. She gave me moral and technical support and her help for me was priceless.

My gratitude goes also to my two thesis reviewers, Dr. Daniel Gitler and Dr. Jasmina Jovanovic for their help to improve my thesis work.

I want to thank Matteo Moschetta, Alessandra Romei, Emanuele Carminati, Antonio De Fusco and Giorgio Grasselli for their help in my PhD project and all my other colleagues for their friendship and love. Despite we are all far from our native home, we built a second family together. Thank you!

Finally, I want to dedicate my PhD work to my family. I would not have been here without their support and their trust.